

CHARACTERIZATION OF THE DISTRIBUTION OF DEVELOPMENTAL
INSTABILITY

By

GREGORY ALAN BABBITT

A DISSERTATION PRESENTED TO THE GRADUATE SCHOOL
OF THE UNIVERSITY OF FLORIDA IN PARTIAL FULFILLMENT
OF THE REQUIREMENTS FOR THE DEGREE OF
DOCTOR OF PHILOSOPHY

UNIVERSITY OF FLORIDA

2006

Copyright 2006

by

Gregory Alan Babbitt

This document is dedicated to my grandmother, Sarah Miller, who taught me to admire
the natural world.

ACKNOWLEDGMENTS

I would like to thank Rebecca Kimball, Susan Halbert, Bernie Hauser, Jane Brockmann, and Christian Klingenberg for helpful discussions and comments; Susan Halbert and Gary Steck (Division of Plant Industry, State of Florida) for specimen ID; Marta Wayne for use of her microscope and digital camera; Glenn Hall (Bee Lab, University of Florida) for a plentiful supply of bees; and the Department of Entomology and Nematology (University of Florida) for use of its environmental chambers. I thank Callie Babbitt for help in manuscript preparation and much additional love and support.

TABLE OF CONTENTS

| | <u>page</u> |
|--|-------------|
| ACKNOWLEDGMENTS | iv |
| LIST OF TABLES | viii |
| LIST OF FIGURES | ix |
| ABSTRACT | xii |
| CHAPTER | |
| 1 SEARCHING FOR A CONSISTENT INTERPRETATION OF DEVELOPMENTAL INSTABILITY? A GENERAL INTRODUCTION | 1 |
| 2 ARE FLUCTUATING ASYMMETRY STUDIES ADEQUATELY SAMPLED? IMPLICATIONS OF A NEW MODEL FOR SIZE DISTRIBUTION | 10 |
| Introduction..... | 10 |
| Developmental Stability: Definition, Measurement, and Current Debate | 10 |
| The Distribution of Fluctuating Asymmetry | 12 |
| Methods | 17 |
| Results..... | 22 |
| Discussion..... | 30 |
| The Distribution of FA | 30 |
| Sample Size and the Estimation of Mean FA..... | 32 |
| The Basis of Fluctuating Asymmetry | 33 |
| Conclusion | 34 |
| 3 INBREEDING REDUCES POWER-LAW SCALING IN THE DISTRIBUTION OF FLUCTUATING ASYMMETRY: AN EXPLANATION OF THE BASIS OF DEVELOPMENTAL INSTABILITY | 36 |
| Introduction..... | 36 |
| What is the Basis of FA? | 36 |
| Exponential Growth and Non-Normal Distribution of FA..... | 38 |
| Testing a Model for the Basis of FA | 40 |
| Methods | 41 |
| Model Development | 41 |
| Simulation of geometric Brownian motion | 41 |

| | |
|---|--------|
| Simulation of fluctuating asymmetry | 44 |
| Inbreeding Experiment | 45 |
| Morphometric analyses | 48 |
| Model selection and inference..... | 49 |
| Results..... | 49 |
| Model Simulation | 49 |
| Experimental Results..... | 50 |
| Model Selection and Inference..... | 52 |
| Discussion..... | 54 |
| Revealing the Genetic Component of FA | 54 |
| Limitations of the Model | 56 |
| The Sources of Scaling..... | 56 |
| Potential Application to Cancer Screening..... | 57 |
| Conclusion..... | 58 |
| 4 TEMPERATURE RESPONSE OF FLUCTUATING ASYMMETRY TO IN AN APHID CLONE: A PROPOSAL FOR DETECTING SEXUAL SELECTION ON DEVELOPMENTAL INSTABILITY..... | 60 |
| Introduction..... | 60 |
| The Genetic Basis of FA | 60 |
| The Environmental Basis of FA..... | 61 |
| Temperature and FA in and Aphid Clone | 63 |
| Methods | 65 |
| Results..... | 68 |
| Discussion..... | 72 |
| 5 CONCLUDING REMARKS AND RECOMMENDATIONS | 75 |
| How Many Samples Are Enough? | 76 |
| What Measure of FA is best?..... | 76 |
| Does rapid growth stabilize or destabilize development? | 78 |
| Can fluctuating asymmetry be a sexually selected trait?..... | 78 |
| Is fluctuating asymmetry a valuable environmental bioindicator? | 79 |
| Scaling Effects in Statistical Distributions: The Bigger Picture..... | 80 |
| APPENDIX | |
| A LANDMARK WING VEIN INTERSECTIONS CHOSEN FOR ANALYSISOF FLUCTUATING ASYMMETRY..... | 84 |
| B USEFUL MATHEMATICAL FUNCTIONS | 86 |
| Asymmetric Laplace Distribution..... | 86 |
| Half-Normal Distribution | 86 |
| Lognormal Distribution | 86 |
| Double Pareto Lognormal Distribution | 86 |

| | |
|---------------------------|----|
| LIST OF REFERENCES..... | 88 |
| BIOGRAPHICAL SKETCH | 96 |

LIST OF TABLES

| <u>Table</u> | <u>page</u> |
|--|-------------|
| 2-1. Maximized log-likelihood (MLL), number of model parameters (P) and Akaike Information Criterion differences (Δ AIC) for all distributional models tested. Winning models have AIC difference of zero. Models with nearly equivalent goodness-of-fit to winners are underscored (Δ AIC <3.0). $4.0 < \Delta$ AIC <7.0 indicates some support for specified model. Δ AIC >10.0 indicates no support (Burnham and Anderson 1998). Distances between landmarks (LM) used for first univariate size FA, aphids LM 1-2, bees LM 1-4 and long-legged fly LM 3-6 and for second univariate FA aphids LM 2-3, bees LM 2-6 and long-legged fly LM 4-5..... | 23 |
| 2-2. Best fit parameters for models in Table 2-1. Parameters for univariate size FA are very similar to multivariate size FA and are not shown. Skew indexes for asymmetric Laplace are also not shown..... | 24 |
| 3-1. Distribution parameters and model fit for multivariate FA in two wild populations and four inbred lines of <i>Drosophila simulans</i> and one isogenic line of <i>Drosophila melanogaster</i> . Model fits are Δ AIC for unsigned centroid size FA (zero is best fit, lowest number is next best fit). | 51 |

LIST OF FIGURES

| <u>Figure</u> | <u>page</u> |
|--|-------------|
| 2-1. Schematic representation of mathematical relationships between candidate models for the distribution of fluctuating asymmetry. Mixtures here are continuous. | 14 |
| 2-2. Distribution of multivariate shape FA of A) cotton aphid (<i>Aphis gossipyii</i>) B) domestic honeybee (<i>Apis mellifera</i>) and C) long-legged fly (<i>Chrysosoma crinitus</i>). Best fitting lognormal (dashed line, lower inset), and double Pareto lognormal (solid line, upper inset) are indicated. | 25 |
| 2-3. Distribution of multivariate centroid size FA of A) cotton aphid (<i>Aphis gossipyii</i>) B) domestic honeybee (<i>Apis mellifera</i>) and C) long-legged fly (<i>Chrysosoma crinitus</i>). Best fitting half-normal (dashed line, lower inset) and double Pareto lognormal distribution (solid line, upper inset) are indicated. | 26 |
| 2-4. Distribution of univariate unsigned size FA of A) cotton aphid (<i>Aphis gossipyii</i>) B) domestic honeybee (<i>Apis mellifera</i>) and C) long-legged fly (<i>Chrysosoma crinitus</i>). Best fitting half-normal (dashed line, lower inset) and double Pareto lognormal distribution (solid line, upper inset) are indicated. | 27 |
| 2-5. Distribution of sample sizes (n) from 229 fluctuating asymmetry studies reported in three recent meta-analyses (Vollestad et al. 1999, Thornhill and Møller 1998 and Polak et al. 2003). Only five studies had sample sizes greater than 500 (not shown). | 28 |
| 2-6. Relationship between sample size and % error for estimates of mean FA drawn from best fitting size (dashed line) and shape (solid line) distributions using 1000 draws per sample size. All runs use typical winning double Pareto lognormal parameters (shape FA $\nu = -3.7$, $\tau = 0.2$, $\alpha = 1000$, $\beta = 9$; for size FA $\nu = 1.2$, $\tau = 0.7$, $\alpha = 4.0$, $\beta = 4.0$). | 29 |
| 2-7. The proportion and percentage (inset) of individuals with visible developmental errors on wings (phenodeviant) are shown for cotton aphids (A) and honeybees (B) in relation to distribution of shape FA (Procrustes distance). Average FA for both normal and phenodeviant aphids (C) and honeybees (D) are also given. | 30 |
| 3-1. Ordinary Brownian motion (lower panel) in N simulated by summing independent uniform random variables (W) (upper panel). | 42 |

| | |
|--|----|
| 3-2. Geometric Brownian motion in N and log N simulated by multiplying independent uniform random variables. This was generated using Equation 1.5 with $C = 0.54$. | 43 |
| 3-3. Geometric Brownian motion in N and log N with upward drift. This was generated using Equation 1.5 with $C = 0.60$. | 44 |
| 3-4. Model representation of Reed and Jorgensen's (2004) physical size distribution model. Variable negative exponentially distributed stopping Times of random proportional growth (GBM with $C = 0.5$) create double Pareto lognormal distribution of size. | 46 |
| 3-5. A model representation of developmental instability. Normally variable stopping times of random proportional growth (GBM with $C > 0.5$) create double Pareto lognormal distribution of size. | 47 |
| 3-6. Simulated distributions of cell population size and FA for different amounts of variation in the termination of growth (variance in normally distributed growth stop time). The fit of simulated data to the normal distribution can determined by how closely the plotted points follow the horizontal line (a good fit is horizontal). | 50 |
| 3-7. Distribution of fluctuating asymmetry and detrended fit to normal for two samples of wild population collected in Gainesville, FL in summers of 2004 and 2005 and four inbred lines of <i>Drosophila simulans</i> derived from eight generations of full-sib crossing of the wild population of 2004. Also included is one isogenic line of <i>Drosophila melanogaster</i> (mel75). All $n = 1000$. The fit of data to the normal distribution can determined by how closely the plotted points follow the horizontal line (a good fit is horizontal). | 53 |
| 4-1. Predicted proximate and ultimate level correlations of temperature and growth rate to fluctuating asymmetry are different. Ultimate level (evolutionary) effects assume energetic limitation of individuals in the system. Proximate level (growth mechanical) effects do not. Notice that temperature and fluctuating asymmetry are negatively correlated in the proximate model while in the ultimate model they are positively correlated. | 64 |
| 4-2. Cotton aphid mean development time ± 1 SE in days in relation to temperature ($n = 531$). | 68 |
| 4-3. Distribution of isogenic size, size based and shape based FA in monoclonal cotton aphids grown in controlled environment at different temperatures. Distributions within each temperature treatment are similar to overall distributions shown here. | 69 |
| 4-4. Mean isogenic FA for (A.) centroid size- based and (B.) Procrustes shape-based) in monoclonal cotton aphids (collected in Gainesville FL) grown on isogenic cotton seedlings at different temperatures. | 70 |

| | |
|--|----|
| 4-5. Kurtosis of size-based FA in monoclonal cotton aphids grown on isogenic cotton seedlings at different temperatures..... | 71 |
|--|----|

Abstract of Dissertation Presented to the Graduate School
of the University of Florida in Partial Fulfillment of the
Requirements for the Degree of Doctor of Philosophy

CHARACTERIZATION OF THE DISTRIBUTION OF DEVELOPMENTAL
INSTABILITY

By

Gregory Alan Babbitt

May 2006

Chair: Rebecca Kimball
Cochair: Benjamin Bolker
Major Department: Zoology

Previous work on fluctuating asymmetry (FA), a measure of developmental instability, has highlighted its controversial relationship with environmental stress and genetic architecture. I suggest that conflict may derive from the fact that the basis of FA is poorly understood and, as a consequence, the methodology for FA studies may be flawed. While size-based measures of FA have been assumed to have half-normal distributions within populations, developmental modeling studies have suggested other plausible distributions for FA. Support for a non-normal distribution of FA is further supported by empirical studies that often record leptokurtic (i.e., fat or long-tailed) distributions of FA as well. In this dissertation, I investigate a series of questions regarding the both the basis and distribution of FA in populations. Is FA normally distributed and therefore likely to be properly sampled in FA studies? If not normal, what candidate model distribution best fits the distribution of FA? Is the shape of the distribution of FA similar to a simple and specific growth model (geometric Brownian

motion)? Does reducing individual variation in populations through inbreeding affect follow the prediction of this model? How does this shape respond to environmental factors such as temperature when genetic variation is controlled?

In three species of insects (cotton aphid, *Aphis gossipyii* Glover; honeybee, *Apis mellifera*; and long-legged fly, *Chrysosoma crinitus* (Dolichopodidae)), I find that FA was best described by a double Pareto lognormal distribution (DPLN), a lognormal distribution with power-law tails. The large variance in FA under this distribution and the scaling in the tails both act to slow convergence to the mean, suggesting that many past FA studies are under-sampled when the distribution of FA is assumed to be normal. Because DPLN can be generated by geometric Brownian motion, it is ideal for describing behavior of cell populations in growing tissue. I demonstrated through both a mathematical growth model and an inbreeding experiment in *Drosophila simulans* that the shape of the distribution of FA is highly dependent on the level of genetic redundancy or heterogeneity in a population. In monoclonal lines of cotton aphids, I also demonstrate that FA decreases with temperature and that a shift in kurtosis is associated with temperature induced phenotypic plasticity. This supports the prediction of a proximate model for the basis of FA and also suggests shape of the distribution of FA responds to environmentally induced changes in gene expression on the same genetic background.

CHAPTER 1

SEARCHING FOR A CONSISTENT INTERPRETATION OF DEVELOPMENTAL INSTABILITY? A GENERAL INTRODUCTION

Everywhere, nature works true to scale and everything has its proper size.
-- D'Arcy Thompson

There have been many incarnations of the idea that stability and symmetry are somehow related. Hippocrates (460-377 B.C.) was the first to postulate internal corrective properties that work in the presence of disease. Waddington (1942) suggested existence of similar homeostatic buffering against random and presumably additive errors occurring during development. The term “fluctuating asymmetry,” first introduced by Ludwig (1932), was later adopted by Mather (1953), Reeve (1960) and Van Valen (1962) to describe a measurable form of morphological noise representing a hypothetical lack of buffering that is always present during development of organisms. Recently, biologists have become very interested both in fluctuating asymmetry’s potential usefulness as a universal bioindicator of environmental health (Parsons 1992) and in its potential as an indicator or even an overt signal of an individual’s overall genetic quality (Møller 1990). However, over a decade of work has left the field with no clear relationship between increased fluctuating asymmetry and either environmental or genetic stress (Bjorksten et al. 2000, Lens et al. 2002). Despite this fact, fluctuating asymmetry is still often assumed to indicate of developmental instability. Recently, Debat and David (2001) page 560 define developmental stability as “a *set of mechanisms* historically selected to *keep the phenotype constant* in spite of *small random developmental irregularities potentially*

inducing slight differences among homologous parts within individuals.” (I have italicized the aspects of this definition that I think are left undefined.)

Fluctuating asymmetry is defined and measured as the average right minus left difference in size or shape of morphological characters in a population and has been generally accepted as an indicator of developmental instability because both sides of a bilaterally symmetric organism have been developed by the same genetic program in the same environment (Møller and Swaddle 1997). Fluctuating asymmetry is measured as left-right side differences in the size or shape of paired bilaterally symmetric biological structures of organisms. In a character trait that demonstrates fluctuating asymmetry, it is assumed that the distribution of signed left–right differences is near zero and that there is no selection for asymmetry (Palmer and Strobek 1986, 2003). Other types of asymmetry do exist and are thought to indicate selection against symmetry. Directional asymmetry denotes a bias towards left or right sidedness that causes the population mean to move away from zero. In antisymmetry, left or right side biases occur equally at the individual level creating a population that is bimodal or platykurtic.

While much attention has been directed toward the possible genetic basis of fluctuating asymmetry (reviewed by Leamy and Klingenberg 2005, Woolf and Markow 2003), response of fluctuating asymmetry to stress (reviewed by Hoffman and Woods 2003) and correlation of fluctuating asymmetry with mate choice (Møller and Swaddle 1997); little scientific effort has been directed toward investigating its basis or origin at levels of organization lower than the individual. A few theoretical explanations for the basis of fluctuating asymmetry have been developed (reviewed by Klingenberg 2003). Only two of these offer a causal explanation for the increased levels of fluctuating

asymmetry that are sometimes observed under periods of environmental stress. While not mutually exclusive, these two explanations differ at the organizational level at which they are thought to act. Møller and Pomiankowski (1993) first suggested that strong natural or sexual selection can remove regulatory steps controlling the symmetric development of certain traits (e.g., morphology used in sexual display). They suggest that with respect to sexually selected traits (and assuming that they are somehow costly to produce), individuals may vary in their ability to buffer against environmental stress in proportion to the size of their own energetic reserves. These reserves are often indicative of the genetic quality of individuals. Therefore, high genetic quality is expected to be associated with low fluctuating asymmetry. Emlen et al. (1993) present another and more proximate explanation of the basis of fluctuating asymmetry. They do not invoke sexual selection but hypothesize that fluctuating asymmetry is due largely to the non-linear dynamics of signaling and supply that may occur during growth. Here fluctuating asymmetry is thought to result from the scaling up of compounding temporal asymmetries in signaling between cells during growth. In their model, hypothetical levels of signaling compounds (morphogens) and or growth precursors used in the construction of cells vary randomly over time. When growth suffers less interruption, in other words, when it occurs faster and under less stress, there is also less complexity (and fractal dimension) in the dynamics of signaling and supply. This should reduce fluctuating asymmetry.

Only a few other models have since been proposed. A model by Graham et al. (1993) suggests that fluctuating asymmetry in the individual can also be the net result of compounding time lags and chaotic behavior between hormonally controlled growth rates

on both sides of an axis of bilateral symmetry. More recently Klingenberg and Nijhout (1999) present a model of morphogen diffusion and threshold response that includes genetic control of each component. They demonstrate that fluctuating asymmetry can result from genetically modulated expression of variation that is entirely non-genetic in origin. In other words, even without specific genes for fluctuating asymmetry, interaction between genetic and non-genetic sources of variation (G x E) can cause fluctuating asymmetry (Klingenberg 2003).

While all these theories for the basis of fluctuating asymmetry have proven useful in making some predictions about fluctuating asymmetry in relation to sexual selection and growth rate/trait size, none are grounded in any known molecular mechanisms. The search for any single molecular mechanism that stabilizes the developmental process has proven elusive. A recent candidate was the heat shock protein, Hsp90, which normally target conformationally plastic proteins that act as signal transducers (i.e., molecular switches) in many developmental pathways (Rutherford and Lundquist 1998). Because Hsp90 recognizes protein folding, it can also be diverted to misfolded proteins that are denatured during environmental stress. Therefore, Hsp90 can potentially link the developmental process to the environment and these authors suggest it may also capacitate the evolution of novel morphology during times of stress by revealing genetic variation previously hidden to selection in non-stressful environments. However, additional research by Milton et al. (2003) shows that while Hsp90 does buffer against a wide range of morphologic changes and does mask the effect of much hidden genetic variation in *Drosophila*, it does not appear to affect average levels of fluctuating asymmetry through any single Hsp90 dependent pathway or process.

It is said that wisdom begins with the naming of things. The case of fluctuating asymmetry reminds us that the act of giving names to things in science can, in fact, lend a false impression that we have achieved a true understanding of that which has been named. While fluctuating asymmetry has had several specific descriptive definitions, we do not really know how to define it at a fundamental level because we do not understand exactly how development is destabilized under certain conditions of both gene and environment. All we can say for now is that fluctuating asymmetry is a mysterious form of morphological variation. Mary Jane West-Eberhard (2003) has dubbed it the “dark side” of variation because it may represent that noisy fraction of the physical-biological interface that is still free of selection, and not under direct control of the gene.

Any study of natural variation would do well to begin by simply observing its shape or its distribution in full. In nature, statistical distributions come mostly in two flavors: those generated by large systems of independent additive components and those generated by large systems of interacting multiplicative components (Vicsek 2001, Sornette 2003). When large systems are composed of independent subunits, random processes result in the normal distribution, the cornerstone of classical statistics. The normal distribution is both unique and extreme in its rapidly decaying tails, its very strong central tendency and its sufficient description by just two parameters, the mean and variance, making it, in this sense, the most parsimonious description of random variation. However, the normal distribution does not describe all kinds of stochastic or random behavior commonly observed in the natural sciences. When subunits comprising large systems interact, random processes are best described by models that underlie statistical physics (sometimes called Levy statistics) (Bardou et al. 2003. Sornette 2003).

Fat-tailed distributions are often the result of propagation of error in the presence of strong interaction. These types of distributions include the power function, Pareto, Zipf and the double Pareto or log-Laplace distributions, all characterized by a power law and an independence of scale. Collective effects in complex interacting systems are also often characterized by these power laws (Wilson 1979, Stanley 1995). Examples include higher order phase transitions, self-organized criticality and percolation. During second order phase transition at the critical temperature between physical phases, external perturbation of the network of microscopic interactions between molecules results in system reorganization at a macroscopic level far above that of interacting molecules (e.g., the change from water to ice). This results in collective imitation that propagates among neighboring molecules over long distances. Exactly at these critical temperatures, imitation between neighbors can be observed at all scales creating regions of similar behavior that occur at all sizes (Wilson 1979). Thus, a self-similar power-law manifests itself in the interacting system's susceptibility to perturbation and results, in this case, from the multiplicity of interaction paths in the interaction network (Stanley 1995). As the distance between two objects in a network increases, the number of potential interaction pathways increases exponentially and the correlation between such paths decreases exponentially. The constant continuous degree of change represented by the power law is the result of a combined effect between both an exponentially increasing and decreasing rate of change. This highlights the fact that power laws can be easily manifested from combinations of exponential functions which are very common to patterns of change in many natural populations (both living and non-living).

Therefore, it is important to note that power laws in statistical distributions do not have to always indicate strong interaction in a system and that many other simple mechanisms can create them (Sornette 2003), especially where the behavior of natural populations are concerned. For example, an apparently common method by which power laws are generated in nature is when stochastic proportional (geometric) growth is observed randomly in time (Reed 2001). Power law size distributions in particle size, human population size, and economic factors are all potentially explained by this process (Reed and Jorgensen 2004). Here we also have exponential increase in size opposing an exponential decrease in the probability of observation or termination that results in a gently decaying power law. This process can also explain why power law scaling can occur through the mixing of certain distributions where locally exponentially increasing and decreasing distributions overlap. For example, superimposing lognormal distributions results in a lognormal distribution with power law tails (Montroll and Shlesinger 1982,1983).

Given that exponential relationships are so common in the natural world, we should assume that in observing any large natural population outside of an experiment, there is probably some potential for a power-law scaling effect to occur. Therefore some degree of non-normal behavior may be likely to be observed, often in the underlying distribution's tail. If we assume an underlying normal distribution, and sample it accordingly, we are likely to under-sample this tail. And so we rarely ever present ourselves with enough data to challenge our assumption of normality, and we risk missing the chance to observe a potentially important aspect of natural variation.

Until now, the basis of fluctuating asymmetry has been addressed only with very abstract models of hypothetical cell signaling, or at the level of selection working on the organism with potential mechanism remaining hypothetical. In this dissertation, the underlying common theme is that fluctuating asymmetry must first and foremost be envisioned as a stochastic process occurring during tissue growth, or in other words, occurring within an exponentially expanding population of cells. This expansion process can be modeled by stochastic proportional (geometric) growth that is terminated or observed randomly over time. As will be explained in subsequent chapters, this generative process can naturally lead to variation that distributes according to a lognormal distribution with power laws in both tails (Reed 2001). In chapter 2, I examine the distribution of fluctuating asymmetry in the wings of three species of insects (cotton aphid, *Aphis gossipyi* Glover, honeybee, *Apis mellifera*, and long-legged flies, *Chrysosoma crinitus*) and test various candidate models that might describe the statistical distribution of fluctuating asymmetry. I then address whether, given the best candidate model, fluctuating asymmetry studies have been appropriately sampled. I suggest that much of the current controversy over fluctuating asymmetry may be due to the fact that past studies have been under-sampled. In chapter 3, I extend and test a phenomenological model for fluctuating asymmetry that is introduced in chapter 2. I present the model and then examine some of its unique predictions concerning the effects of inbreeding on the shape of the distribution of fluctuating asymmetry in *Drosophila*. I present evidence that the genetic structure of a population can have a profound effect on the scaling and shape of the observed distribution of fluctuating asymmetry. In chapter 4, I characterize the pattern of developmental noise (fluctuating asymmetry in the absence

of genetic variation) in two monoclonal populations of cotton aphid cultured under graded environmental temperatures. I investigate how developmental noise is altered by this simple change in the environment. I present evidence that the environmental response of size-based FA is directly related to developmental time. Lastly, I conclude with a review of my major findings in the context of the introduction I have presented here.

CHAPTER 2

ARE FLUCTUATING ASYMMETRY STUDIES ADEQUATELY SAMPLED? IMPLICATIONS OF A NEW MODEL FOR SIZE DISTRIBUTION

Introduction

Developmental Stability: Definition, Measurement, and Current Debate

Developmental stability is maintained by an unknown set of mechanisms that buffer the phenotype against small random perturbations during development (Debat and David 2001). Fluctuating asymmetry (FA), the most commonly used assay of developmental instability, is defined either as the average deviation of multiple traits within a single individual (Van Valen 1962) or the deviation of a single trait within a population (Palmer and Strobek 1986, 2003; Parsons 1992) from perfect bilateral symmetry. Ultimately, an individual's developmental stability is the collective result of random noise, environmental influences, and the exact genetic architecture underlying the developmental processes in that individual (Klingenberg 2003; Palmer and Strobek 1986). Extending this to a population, developmental stability is the result of individual variation within each of these three components.

Currently, there is conflict in the literature regarding the effect of both environment and genes on the developmental stability of populations. The development of bilateral symmetry appears to be destabilized to various degrees by both environmental stressors (review in Møller and Swaddle 1997) and certain genetic architectures (usually created by inbreeding: Graham 1992; Lerner 1954; Mather 1953; Messier and Mitton 1996; review by Mitton and Grant 1984). While the influence of inbreeding on FA is not

consistent (Radwan 2003; Carchini et al. 2001; Fowler and Whitlock 1994; Leary et al. 1983, 1984; Lens et al. 2002; Perfectti and Camachi 1999; Rao et al. 2002; Vollestad et al. 1999), it has led biologists to use terminology such as “genetic stress” or “developmental stress” when describing inbred populations (Clarke et al. 1986 and 1993; Koehn and Bayne 1989; Palmer and Strobek 1986).

While genetic and environmental stressors have been shown to contribute to developmental instability and FA, the full picture is still unclear (Bjorksten et al. 2000; Lens et al. 2002). While FA has been proposed as a universal indicator of stress within individual organisms (Parsons 1992), its utility as a general indicator of environmental stress has been contentious (Bjorksten et al. 2000; Ditchkoff et al. 2001; McCoy and Harris 2003; Merila and Bjorklund 1995; Møller 1990; Rasmuson 2002; Thornhill and Møller 1998; Watson and Thornhill 1994; Whitlock 1998). Despite many studies, no clear general relationship between environmental stress and FA has been demonstrated or replicated through experimentation across different taxa (Bjorksten et al. 2000; Lens et al. 2002). Furthermore, the effects of stress on FA appear to be not only species-specific but also trait-specific and stress-specific (Bjorksten et al. 2000). Several meta-analyses have attempted to unify individual studies on the relation of sexual selection, heterozygosity, and trait specificity to FA (Polak et al. 2003; Thornhill and Møller 1998; Vollestad et al. 1999); while some weak general effects have been found, their biological significance is still unresolved.

Taken together, the ambiguity of the results from FA studies suggests unresolved problems regarding the definition and/or measurement of FA. The distribution and overall variability of FA are sometimes discussed with regards to repeatability in FA

studies (Whitlock 1998; Palmer and Strobeck 2003), but is seldom a primary target of investigation. Until we can quantify FA more reliably and understand its statistical properties, the potential for misinterpretation of FA is likely to persist.

The Distribution of Fluctuating Asymmetry

Although it is always risky to infer underlying processes from observed patterns, careful examination of the distribution of FA in large samples may help distinguish between possible scenarios driving FA. For instance, a good fit to a single statistical distribution may imply that the same process operates to create FA in all individuals in a population. In contrast, a good fit to a discrete mixture of several different density functions might suggest that highly asymmetric individuals suffer from fundamentally different developmental processes than their more symmetric counterparts. Thin-tailed distributions (e.g., normal or exponential) may indicate relative independence in the accumulation of small random developmental errors, whereas heavy-tailed distributions may implicate non-independent cascades in the propagation of such error. Despite much interest in the relationship between environmental stress and levels of FA, the basic patterns of its distribution in populations remain largely unexplored.

One common distributional attribute of FA, leptokurtosis, has been discussed in the literature. Leptokurtosis denotes a distribution that has many small and many extreme values, relative to the normal distribution. Two primary causes of this kind of departure from the normal distribution are the mixing of distributions and/or scaling effects in data. For example, the Laplace or double exponential distribution is leptokurtic (but not heavy-tailed) and can be represented as a continuous mixture of normal distributions (Kotz et al. 2001; Kozubowski and Podgorski 2001). Just as log scaling in the normal distribution results in the lognormal distribution, log scaling in the Laplace leads to log-Laplace (also

called double Pareto) distributions (Kozubowski and Podgorski 2002; Reed 2001), which are both leptokurtic and heavy-tailed (see Figure 2-1). Several explanations for leptokurtosis in the distribution of FA have been proposed. Both individual differences in developmental stability within a population (Gangestad and Thornhill 1999) and differences in FA between subpopulations (Houle 2000) have been suggested to lead to continuous or discrete mixtures of normal distributions with different developmental variances, which in turn would cause leptokurtosis (e.g., a Laplace distribution) in the overall distribution of FA. Mixtures of non-normal distributions may also cause either leptokurtosis or platykurtosis (more intermediate values than the normal distribution: Palmer and Strobek 2003). A potential example of this is illustrated by Hardersen and Frampton's (2003) demonstration that a positive relationship between mortality and asymmetry can cause leptokurtosis. Alternatively, Graham et al. (2003) have argued that developmental error should behave multiplicatively in actively growing tissues, creating a lognormal size distribution in most traits rather than the normal distribution that is usually assumed. They argue that this ultimately results in leptokurtosis (but not fat tails) and size dependent expression of FA. Because simple growth models are often geometric, we should not be surprised if distributions of size-based FA followed the lognormal distribution (see Limpert et al. 2001 for a review of lognormal distributions in sciences).

Not well recognized within biology is the fact that close interaction of many components can result in power-law scaling (distributional tails that decrease proportional to x^{-a} rather than to some exponential function of x such as $\exp(-ax)$ [exponential] or $\exp(-ax^2)$ [normal] and hence to heavy-tailed distributions (Sornette 2003). Power-law scaling is often associated with the tail of the lognormal distribution,

especially when log standard deviation is large (Mitzenmacher unpublished ms.;
Montroll and Shlesinger 1982, 1983; Roman and Porto 2001; Romeo et al. 2003).

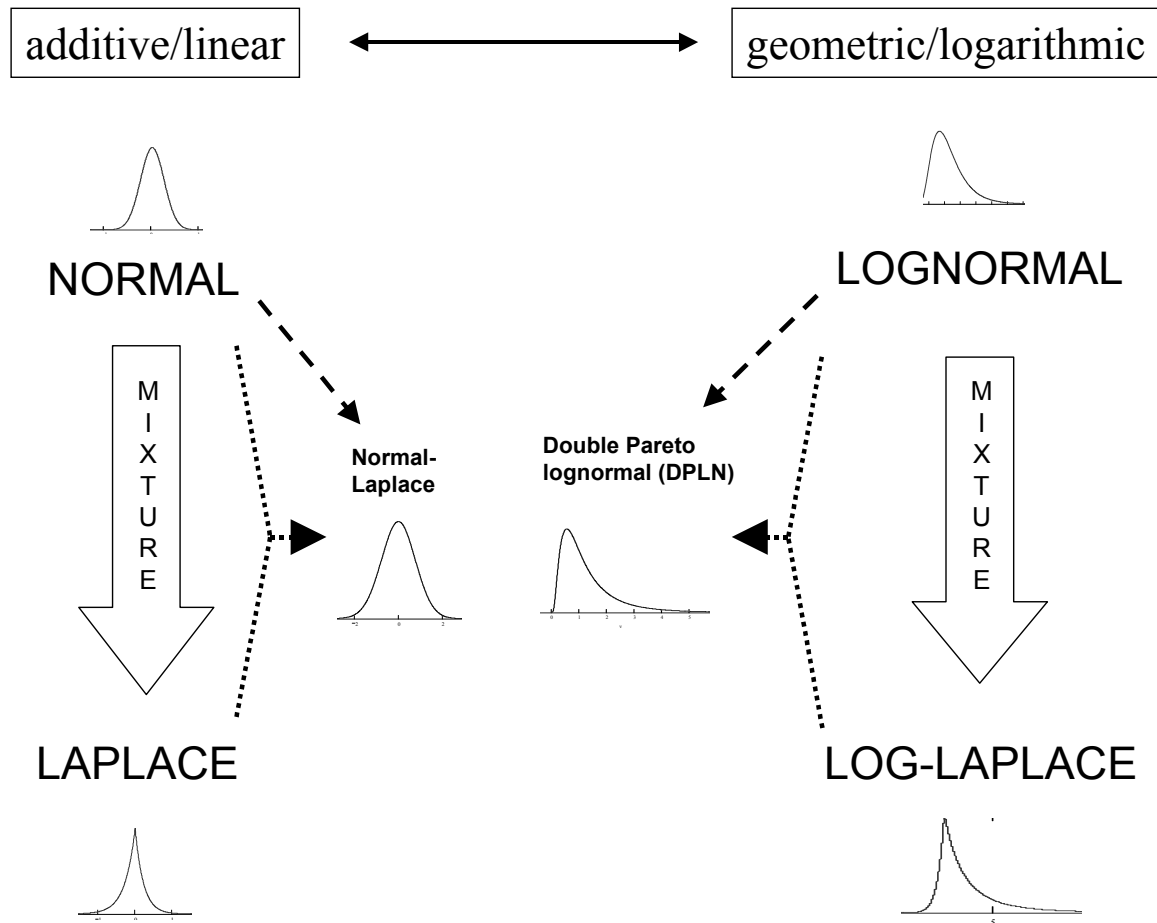


Figure 2-1. Schematic representation of mathematical relationships between candidate models for the distribution of fluctuating asymmetry. Mixtures here are continuous.

KEY:

Solid line – scale of variable ($x \leftrightarrow \ln(x)$)

Dashed line – random walk observed at constant stopping rate (i.e., negative exponentially distributed stop times) Note: random walk on log scale exhibits geometric Brownian motion

Dotted line – convolution of two distributions (one of each type)

Block arrow – a continuous mixture of distributions with stochastic (exponentially distributed) variance

(Note – Log-Laplace is also called double Pareto by Reed 2001, Reed and Jorgensen 2004)

Because FA in a population may reflect fundamental developmental differences between different classes or groups of individuals, for example stressed and non-stressed, or between different subpopulations as suggested by Houle (2000), we might expect discrete mixtures of different distributions to best describe FA. For instance, extreme individuals falling in a heavy upper tail may be those who have exceeded some developmental threshold. Major disruption of development, resulting in high FA, may also reveal the scaling that exists in the underlying gene regulatory network (Albert and Barabasi 2002; Clipsham et al. 2002; Olvai and Barabasi 2002). Alternatively, if FA is produced by a single process, but to various degrees in different individuals, then one might expect a continuous mixture model to best describe the distribution of FA.

The possibility of non-normal distribution of FA opens the door to several potential sampling problems. For instance, if the lognormal shape, or multiplicative variance parameter, is large, then broad distribution effects may slow the convergence of the sample mean to the population mean as sample sizes are increased (Romeo et al. 2003). An additional, thornier, problem is caused by power-law scaling in the tails of distributions. Many lognormally distributed datasets exhibit power-law scaling (or amplification) in the tail region (Montroll and Shlesinger 1982, 1983; Romeo et al. 2003; Sornette 2003), sometimes called Pareto–Levy tails or just Levy tails. As sample sizes grow infinitely large, power-law and Pareto distributions may approach infinite mean (if the scaling exponent is less than three) and infinite variance (if the scaling exponent is less than two), and therefore will not obey the Law of Large Numbers (that sample means approach the population mean as sample sizes increase). Increased sampling actually increases the likelihood of sampling a larger value in the tail of a Pareto distribution

(Bardou et al. 2003; Quandt 1966), creating more uncertainty in estimates of the mean as sample size increases. The presence of power-law tails can slow overall convergence considerably even in distributions that are otherwise lognormal with low variance (which may not look very different from well-behaved lognormal distributions unless a large amount of data is accumulated).

This discussion points to two effects that need to be assessed – broad distribution effects, controlled by the shape (lognormal variance) parameter of the body of the FA distribution, and power-law tails, controlled by the scaling exponents of the tails of the FA distribution. To assess these effects, I apply a new statistical model, the double Pareto lognormal (DPLN) distribution (Reed and Jorgensen 2004). The DPLN distribution is a lognormal distribution with power-law behavior in both tails (for values near zero and large positive values). Similar to the log-Laplace distributions, the DPLN distribution can be represented as a continuous mixture of lognormal distributions with different variances. It can also be derived from a geometric Brownian motion (a multiplicative random walk) that is stopped or “killed” at a constant rate (i.e., the distribution of stop times is exponentially distributed: Reed and Jorgensen 2004; Sornette 2003). The parameters of the DPLN distribution include a lognormal mean (ν) and variance (τ^2) parameter which control the location and spread of the body of the distribution, and power-law scaling exponents for the left (β) and right (α) tails. Special cases of the DPLN include the right Pareto lognormal (RPLN) distribution, with a power-law tail on the right but not the left side ($\beta \rightarrow \infty$); the left Pareto lognormal (LPLN) distribution, with a power-law tail only near zero ($\alpha \rightarrow \infty$); and the lognormal distribution, with no power-law tails ($\alpha \rightarrow \infty, \beta \rightarrow \infty$). For comparison, I also fit normal and half-normal

distributions as well as the asymmetric Laplace distribution to the data on FA. See Figure 2-1 for schematic representation of relationships between these candidate models for FA.

In the following study, I directly test the fit of different distributions to large FA datasets from three species of insects. I include a lab cultured monoclonal line of cotton aphid, *Aphis gossipyii* Glover, in an attempt to isolate the distribution of developmental noise for the first time. I also analyze data from a semi-wild population of domestic honeybee, *Apis mellifera*, taken from a single inseminated single queen colony, and from a large sample of unrelated wild-trapped Long-legged flies (*Chrysosoma crinitus*: Dolichopodidae).

I address two primary groups of goals in this study. First, I investigate what distributions fit FA data best and how the parameters of these distributions vary across species, rearing conditions, and levels of genetic relatedness. I also address whether “outliers” (individuals with visible developmental errors) appear to result from discrete or continuous processes. Secondly, I determine how accurate the estimates of population mean FA are at various sample sizes to determine whether past studies of FA been adequately sampled to accurately estimate mean or average FA in populations. In addition to these two primary goals, I also compare the best-fitting distributions and level of sampling error for three of the most common methods of measuring FA: a univariate and a multivariate size-based metric of asymmetry, and a multivariate shape-based method.

Methods

Wings were collected and removed from three populations of insects and dry mounted on microscope slides. These populations included a monoclonal population of

1022 Cotton Aphid (*Aphis gossipyii* Glover) started from a single individual collected from citrus in Lake Alfred, Florida, 1001 honeybees *Apis mellifera*, maintained at University of Florida and 889 long-legged flies (*Chrysosoma crinitus* :Dolichopodidae). All species identifications were made through the State of Florida Department of Plant Industry in Gainesville and voucher specimens remain available in their collections.

Aphid cultures were maintained on potted plants in reach-in environmental chambers at 15°C with constant 14/10 hour LD cycle generated by 4 – 20 watt fluorescent Grolux brand bulbs. Aphid cultures were cultured on approximately 10 day old cotton seedlings (*Gossipium*) and allowed to propagate until crowded. Crowding stimulated alate formation (winged forms) in later generations which were collected every twenty days with a fine camel hair brush wetted in ethanol. New plants were added every ten days and alates were allowed to move freely from plant to plant starting new clones until they were collected. The temperature at which the colony was maintained created a low temperature “dark morph” Cotton Aphid which still propagated on host plants quickly but was larger than high temperature “light morphs” that form at temperatures greater than 17°C. Dark morphs colonize stems on cotton whereas light morphs colonized the undersides of leaves.

The bees were collected in June 2004 by Dr. Glenn Hall at the University of Florida’s Bee Lab from a single inseminated single queen colony. They were presumably all foragers and haplodiploid sisters collected as they exited the hive into a collection bag. The bag was frozen for three hours and then the bees were placed in 85% ethanol.

Long-legged flies were trapped from a wild population using 14 yellow plastic water pan traps in southwest Gainesville, Florida, during May 2003 and May-June 2004.

A very small amount of dishwashing detergent was added to the water to eliminate surface tension and enhance trapping. Traps were checked every three hours during daylight and set up fresh every day of trapping.

All insect specimens were dried in 85% ethanol, and then pairs of wings were dissected (in ethanol) and air-dried to the glass slides while the ethanol evaporated. Permunt was used to attach cover slips. This technique prevented wings from floating up during mounting, which might slightly distort the landmark configuration. Dry mounts were digitally photographed. All landmarks were identified as wing vein intersections on the digital images (six landmarks on each wing for aphids, eight for honeybees and Dolichopodid flies). See Appendix A for landmark locations on wings for each species.

Wing vein intersections were digitized three times each on all specimens using TPSDIG version 1.31 (Rohlf, 1999). All measures of FA were taken as the average FA value of the three replicate measurements for each specimen. Specimens damaged at or near any landmarks were discarded. Fluctuating asymmetry was measured in three ways on all specimens. First, a common univariate metric of absolute unsigned asymmetry was taken for two different landmarks: $FA = \text{abs}(R - L)$ where R and L are the Euclidean distances between the same two landmarks on either wing. In aphids, landmarks 1-2 and 2-3 were used; in bees, landmarks 1-4 and 2-6 were used; and in long-legged flies, landmarks 3-6 and 4-5 were used. Two multivariate geometric morphometrics using landmark-based methods were performed using all landmarks shown in Appendix A. A multivariate size-based FA (FA 1 in Palmer and Strobek 2003) was calculated as absolute value of $(R - L)$ where R and L are the centroid sizes of each wing (i.e., the average of

the distances of each landmark to their combined center of mass or centroid location). In addition, a multivariate shape-based measure of FA known as the Procrustes distance was calculated as the square root of the sum of all squared Euclidean distances between each left and right landmark after two-dimensional Procrustes fitting of the data (Bookstein 1991; Klingenberg and McIntyre 1998; FA 18 in Palmer and Strobeck 2003; Smith et al. 1997). Procrustes fitting is a three step process including a normalization for centroid size followed by superimposition of two sets of landmarks (right and left) and rotation until all distances between each landmark set is minimized. Centroid size calculation, Euclidean distance calculation and Procrustes fitting were performed using Øyvind Hammer's Paleontological Statistics program PAST version 0.98 (Hammer 2002). For assessing measurement error (ME) of FA (or more specifically, the digitizing error), we conducted a Procrustes ANOVA (in Microsoft Excel) on all pairs of wing images resampled three times each for every species (Klingenberg and McIntyre 1998). Percent measurement error was computed as $(ME/\text{average FA}) \times 100$ where

$$ME = (|FA1 - FA2| + |FA2 - FA3| + |FA1 - FA3|) / 3.$$

All subsequent statistical analyses were performed using SPSS Base 8.0 statistical software (SPSS Inc.).

The fits of all measures of FA to eight distributional models (normal, half-normal, lognormal, asymmetric Laplace, double Pareto lognormal (DPLN), two limiting forms of DPLN, the right Pareto lognormal (RPLN) and the left Pareto lognormal (LPLN) and a discrete mixture of lognormal and Pareto) were compared by calculating negative log likelihoods and Likelihood Ratio Test (LRT) if models were nested and Akaike Information Criteria (AIC) if not nested (Burnham and Anderson 1998; Hilborn and Mangel 1998). Both of these approaches penalize more complex models (those with

more parameters) when selecting the best-fit distributional model for a given dataset. (The Likelihood Ratio Test does not technically apply when the nesting parameter is at the boundary of its allowed region, e.g., when $\alpha \rightarrow \infty$ for the DPLN, but Pinheiro and Bates (2000) suggest that the LRT is conservative, favoring simpler models, under these conditions.) Best fitting parameters were obtained by maximizing the log-likelihood function for each model (Appendix B). The maximization was performed using the conjugate gradient method within unconstrained solve blocks in the program MathCad by MathSoft Engineering and Education Inc (2001), and was also confirmed using Nelder-Mead simplex algorithm or quasi-Newton methods in R version 2.0.1 (2003), a programming environment for data analysis and graphics.

Phenodeviantes were defined as individuals demonstrating missing wing veins, extra wing veins or partial wing veins on either one or both wings. All phenodeviantes in honeybees involved absence of the vein at landmark 6 (LM 6). Phenodeviantes in aphids were more variable but mostly involved absence of wing vein intersections at LM 2 or LM 3. Procrustes distances were estimated for phenodeviantes by omitting the missing landmarks (caused by the phenodeviance) and controlling for the effect of this removal on the sums of squares. I added an average of the remaining sums of squares in place of the missing sums of squares so that the calculated Procrustes distance is comparable to normal specimens (i.e., six landmarks). In almost all phenodeviantes, this involved omission of only one set of landmark values. The frequency of phenodeviantes was examined across the range of the FA distribution (i.e., Procrustes distance), and mean values of the FA for phenodeviantes were compared to normal individuals in order to

assess whether phenodeviants tended to show higher than normal levels of FA in characters that were not affected by the missing, partial, or extra wing veins.

The best fitting parameters of the best fitting models were used to build a distributional model under which repeated sampling was simulated at various sample sizes. Average error in estimation of the mean FA was calculated as a coefficient of variation ($(s / \bar{x}) * 100$) for 1,000 randomly generated datasets. Lastly, comparison were made of the estimation errors given the best fitting distributions of FA to a distribution of sample sizes from 229 FA studies published in three recent meta-analyses (Polak et al. 2003; Thornhill and Møller 1998; Vollestad et al. 1999).

Results

In the distributions of shape-based FA in monoclonal cotton aphids ($n = 1022$), domesticated honeybees ($n = 1001$), and wild trapped long-legged flies ($n = 889$), AIC and LRTs always favored DPLN or RPLN models by a large margin. All size-based FA distributions favored DPLN or LPLN by a large margin (Table 2-1). All variants of discrete mixture models we tried had very poor results (data not shown). Figures 2-2 through 2-4 demonstrate best fitting models for multivariate shape FA (DPLN and lognormal), multivariate centroid size FA (DPLN and half-normal), and univariate size FA (DPLN and half-normal) for all three species. FA was often visually noticeable in aphids, where the mean shape FA (Procrustes distance) was three times higher (0.062 ± 0.00050) than in bees (0.023 ± 0.00026) or flies (0.019 ± 0.00028). I note that distribution of size FA in aphids and bees fit half-normal distribution in the upper tails fairly well but fit relatively poorly among individuals with low FA. Long-legged flies exhibit poor fit to half-normal in both tails.

Table 2-1. Maximized log-likelihood (MLL), number of model parameters (P) and Akaike Information Criterion differences (Δ AIC) for distributional models tested. Winning models have Δ AIC zero. Models with goodness-of-fit nearly equal to winners are underscored (Δ AIC <3.0). $4.0 < \Delta$ AIC <7.0 indicates some support for specified model. Δ AIC >10.0 indicates no support (Burnham and Anderson 1998). Distances between landmarks for first univariate size FA, aphids LM 1-2, bees LM 1-4 and long-legged fly LM 3-6 and for second univariate FA aphids LM 2-3, bees LM 2-6 and long-legged fly LM 4-5.

| Species/model | | Multivariate shape FA | | Multivariate size FA | | First univariate size FA | | Second univariate size FA | |
|-------------------------------|----------|-----------------------|---------------------------------------|----------------------|---------------------------------------|--------------------------|---------------------------------------|---------------------------|---------------------------------------|
| <u>Cotton Aphid</u> | P | <u>MLL</u> | <u>Δ AIC</u> | <u>MLL</u> | <u>Δ AIC</u> | <u>MLL</u> | <u>Δ AIC</u> | <u>MLL</u> | <u>Δ AIC</u> |
| DPLN | 4 | 255.117 | 0.000 | 542.906 | <u>1.236</u> | 545.725 | <u>2.815</u> | 614.123 | <u>2.333</u> |
| RPLN | 3 | 264.72 | 17.207 | 547.44 | 8.303 | 549.789 | 8.944 | 617.498 | 7.083 |
| LPLN | 3 | 256.723 | <u>1.213</u> | 543.288 | 0.000 | 545.317 | 0.000 | 613.957 | 0.000 |
| LNORM | 2 | 734.726 | 955.218 | 1261 | 1433 | 1265 | 1438 | 1413 | 1596 |
| NORM | 2 | 2241 | 3968 | 2847 | 4606 | 3352 | 5612 | 3534 | 5838 |
| HNORM | 1 | 3523 | 6530 | 2370 | 3650 | 2893 | 4691 | 3047 | 4862 |
| LAPLACE | 3 | 637.044 | 761.855 | 1638 | 2189 | 1883 | 2676 | 1950 | 2671 |
| <u>Honey Bee</u> | | | | | | | | | |
| DPLN | 4 | 132.908 | 7.369 | 536.278 | <u>2.744</u> | 454.337 | 0.000 | 515.93 | 6.329 |
| RPLN | 3 | 130.224 | 0.000 | 549.641 | 27.47 | 460.51 | 10.346 | 525.675 | 23.82 |
| LPLN | 3 | 136.361 | 12.275 | 535.906 | 0.000 | 455.483 | <u>0.292</u> | 513.765 | 0.000 |
| LNORM | 2 | 523.667 | 784.888 | 1262 | 1451 | 1081 | 1249 | 1211 | 1393 |
| NORM | 2 | 3371 | 6480 | 2180 | 3286 | 1709 | 2505 | 2302 | 3574 |
| HNORM | 1 | 5319 | 10370 | 1775 | 2475 | 2687 | 1771 | 1924 | 2816 |
| LAPLACE | 3 | 1148 | 2036 | 1387 | 1703 | 1162 | 1413 | 1445 | 1863 |
| <u>Long-legged Fly</u> | | | | | | | | | |
| DPLN | 4 | 146.603 | 37.971 | 452.728 | 0.000 | 453.958 | 0.000 | 412.007 | 0.000 |
| RPLN | 3 | 128.617 | 0.000 | 454.056 | 0.656 | 460.261 | 10.606 | 422.993 | 20.182 |
| LPLN | 3 | 149.585 | 41.935 | 455.818 | 4.18 | 456.237 | <u>2.559</u> | 412.902 | <u>0.212</u> |
| LNORM | 2 | 506.553 | 753.871 | 1055 | 1201 | 1064 | 1216 | 985.894 | 1144 |
| NORM | 2 | 2985 | 5710 | 1760 | 2610 | 1806 | 2701 | 1668 | 2508 |
| HNORM | 1 | 5147 | 10030 | 1084 | 1256 | 1252 | 1590 | 1099 | 1368 |
| LAPLACE | 3 | 1041 | 1825 | 940.241 | 973.02 | 1016 | 1121 | 997.28 | 1169 |

For multivariate shape analysis, right tail power-law exponents (α) were very high (thousands), left-tail exponents (β) from 3.9-9.9, while the dispersion parameter (τ) was narrowly distributed from 0.310 to 0.356. Thus, shape FA exhibited little scaling in tails (i.e., nearly lognormal). For size-based FA, dispersion was much larger (0.57-0.74), and power-law exponents more variable for univariate and multivariate size-based FA (left

tail (β) and right tail (α) were generally low, indicating moderate power-law scaling in both tails) as shown in Table 2-2.

Table 2-2. Best fit parameters for models in Table 1. Parameters for univariate size FA are very similar to multivariate size FA and are not shown. Skew indexes for asymmetric Laplace are also not shown.

| Multivariate shape FA | | | | | Multivariate size FA | | | |
|------------------------|-----------------|--------------------|-------------------|-------------|----------------------|--------------------|-------------------|-------------|
| <u>Cotton</u> | <u>Location</u> | <u>Dispersion/</u> | <u>Right tail</u> | <u>Left</u> | <u>Location</u> | <u>Dispersion/</u> | <u>Right tail</u> | <u>Left</u> |
| <u>Aphid</u> | | <u>Shape</u> | | <u>Tail</u> | | <u>Shape</u> | | <u>Tail</u> |
| DPLN | -2.62 | 0.356 | 1160 | 4.04 | 1.45 | 0.735 | 6.24 | 3.01 |
| RPLN | -3.01 | 0.415 | 7.03 | ∞ | 1.07 | 0.800 | 4.58 | ∞ |
| LPLN | -2.62 | 0.353 | ∞ | 3.90 | 1.73 | 0.699 | ∞ | 2.23 |
| LNORM | -2.87 | 0.434 | - | - | 1.28 | 0.824 | - | - |
| NORM | 0.062 | 0.027 | - | - | 4.92 | 3.94 | - | - |
| HNORM | 0.009 | 0.059 | - | - | 0.163 | 6.31 | - | - |
| LAPLACE | 0.049 | 0.058 | - | - | 0.657 | 2.19 | - | - |
| <u>Honey Bee</u> | | | | | | | | |
| DPLN | -3.74 | 0.310 | 8380 | 9.80 | 1.32 | 0.565 | 10.4 | 1.57 |
| RPLN | -4.02 | 0.274 | 5.52 | ∞ | 0.571 | 0.829 | 4.82 | ∞ |
| LPLN | -3.71 | 0.305 | ∞ | 7.75 | 1.52 | 0.510 | ∞ | 1.35 |
| LNORM | -3.84 | 0.327 | - | - | 0.777 | 0.850 | - | - |
| NORM | 0.023 | 0.008 | - | - | 2.95 | 2.14 | - | - |
| HNORM | 0.007 | 0.018 | - | - | 0.078 | 3.64 | - | - |
| LAPLACE | 0.021 | 0.018 | - | - | 0.550 | 2.24 | - | - |
| <u>Long-legged Fly</u> | | | | | | | | |
| DPLN | -3.93 | 0.346 | 4940 | 10.3 2 | -0.067 | 0.683 | 3.09 | 5.14 |
| RPLN | -4.28 | 0.231 | 3.73 | ∞ | -0.302 | 0.698 | 2.75 | ∞ |
| LPLN | -3.92 | 0.341 | ∞ | 9.91 2 | 0.319 | 0.743 | ∞ | 3.85 |
| LNORM | -4.02 | 0.351 | - | - | 0.060 | 0.783 | - | - |
| NORM | 0.019 | 0.008 | - | - | 2.00 | 2.24 | - | - |
| HNORM | 0.007 | 0.015 | - | - | 0.075 | 2.11 | - | - |
| LAPLACE | 0.017 | 0.017 | - | - | 0.346 | 1.06 | - | - |

Figure 2-5 shows the distribution of FA sample sizes from 229 studies published in three recent meta-analyses (Polak et al. 2003; Thornhill and Møller 1998; Vollestad et al. 1999).

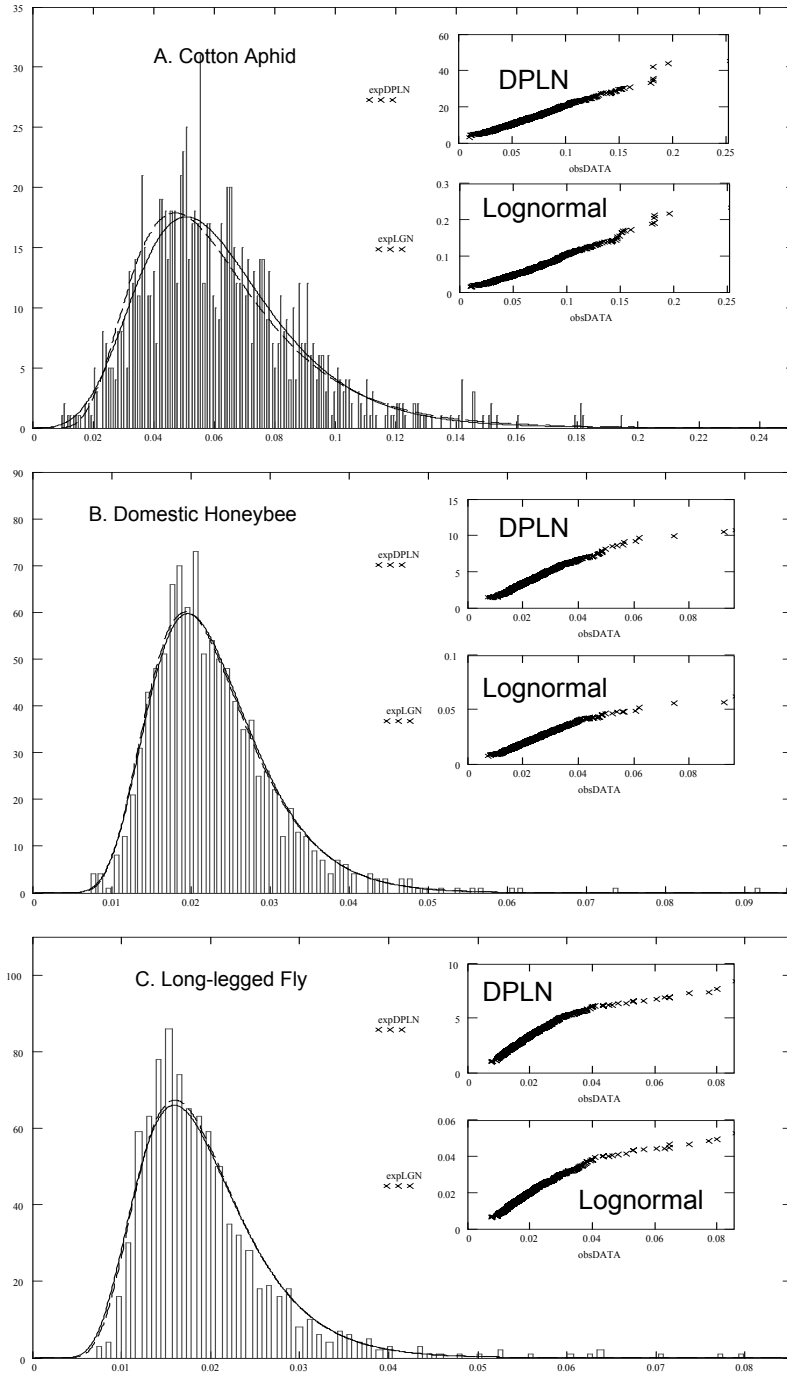


Figure 2-2. Distribution of multivariate shape FA of A) cotton aphid (*Aphis gossipyii*) B) domestic honeybee (*Apis mellifera*) and C) long-legged fly (*Chrysosoma crinitus*). Best fitting lognormal (dashed line, lower inset), and double Pareto lognormal (solid line, upper inset) are indicated.

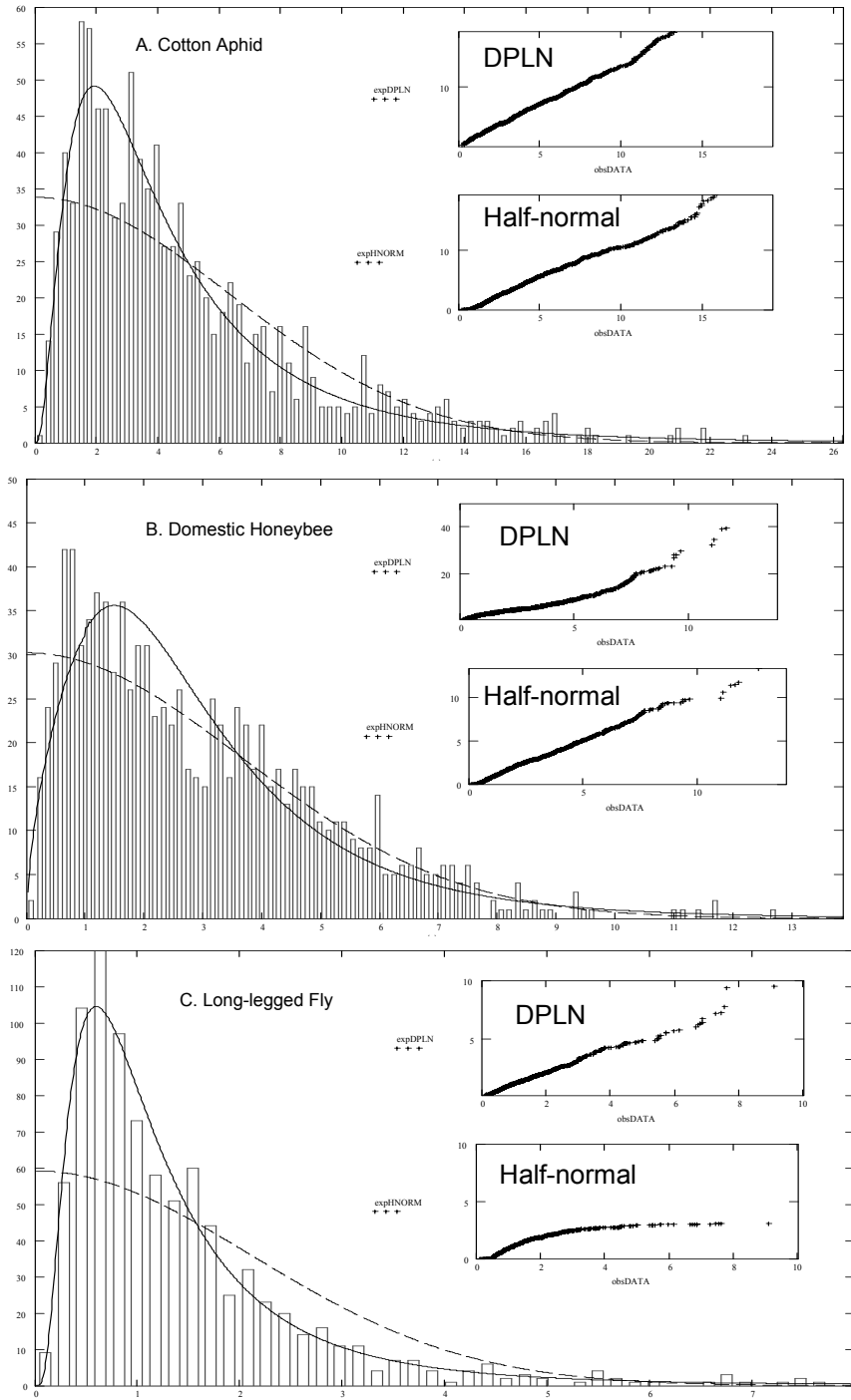


Figure 2-3. Distribution of multivariate centroid size FA of A) cotton aphid (*Aphis gossypii*) B) domestic honeybee (*Apis mellifera*) and C) long-legged fly (*Chrysosoma crinitus*). Best fitting half-normal (dashed line, lower inset) and double Pareto lognormal distribution (solid line, upper inset) are indicated.

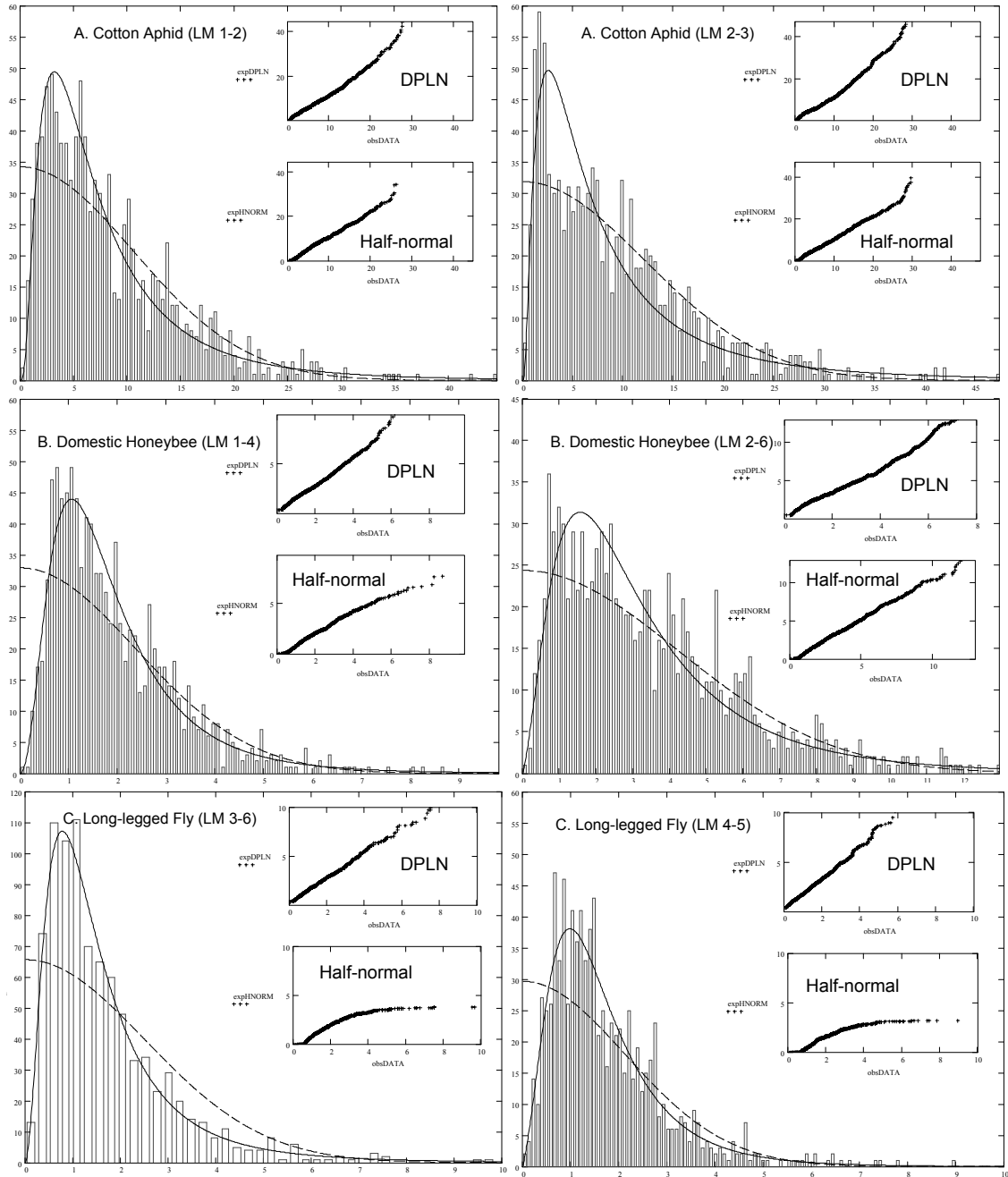


Figure 2-4. Distribution of univariate unsigned size FA of A) cotton aphid (*Aphis gossypii*) B) domestic honeybee (*Apis mellifera*) and C) long-legged fly (*Chrysosoma crinitus*). Best fitting half-normal (dashed line, lower inset) and double Pareto lognormal distribution (solid line, upper inset) are indicated.

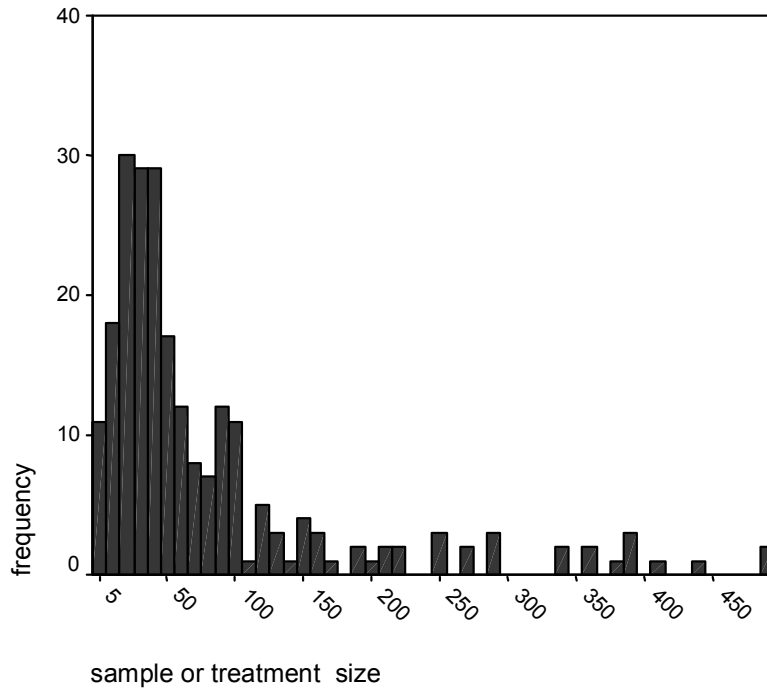


Figure 2-5. Distribution of sample sizes (n) from 229 fluctuating asymmetry studies reported in three recent meta-analyses (Vollestad et al. 1999, Thornhill and Møller 1998 and Polak et al. 2003). Only five studies had sample sizes greater than 500 (not shown).

Nearly 70% of the 229 FA studies have sample or treatment sizes less than 100.

Figure 2-6 demonstrates the hypothetical error levels (coefficients of variations) in estimated mean FA at various sample sizes. Approximate best fit parameters were used to estimate the coefficient of variation (CV) under the DPLN distribution (for shape FA, $\nu = -3.7$, $\tau = 0.35$, $\alpha = 1000$, $\beta = 9$; for size FA, $\nu = 1.2$, $\tau = 0.70$, $\alpha = 4.0$, $\beta = 4.0$). For the same set of landmarks, multivariate shape FA measures lead to the least amount of error in estimating mean FA under DPLN at any sample size. Both univariate and multivariate size FA perform more poorly in terms of both convergence and overall percentage error.

I found that while phenodeviants occurred in almost all regions of the distribution range of FA, the percentage of phenodeviant individuals increased dramatically with

increasing FA (Figure 2-7; aphids, $r = 0.625$ $p = 0.013$; bees, $r = 0.843$ $p = 0.001$). I also found that individuals with phenodeviant wings (both aphids and bees) showed significantly higher levels of FA across those wing landmarks unaffected by the phenodeviant traits ($p < 0.002$ in both aphids and bees). Only a single case of phenodeviance was sampled in long-legged flies.

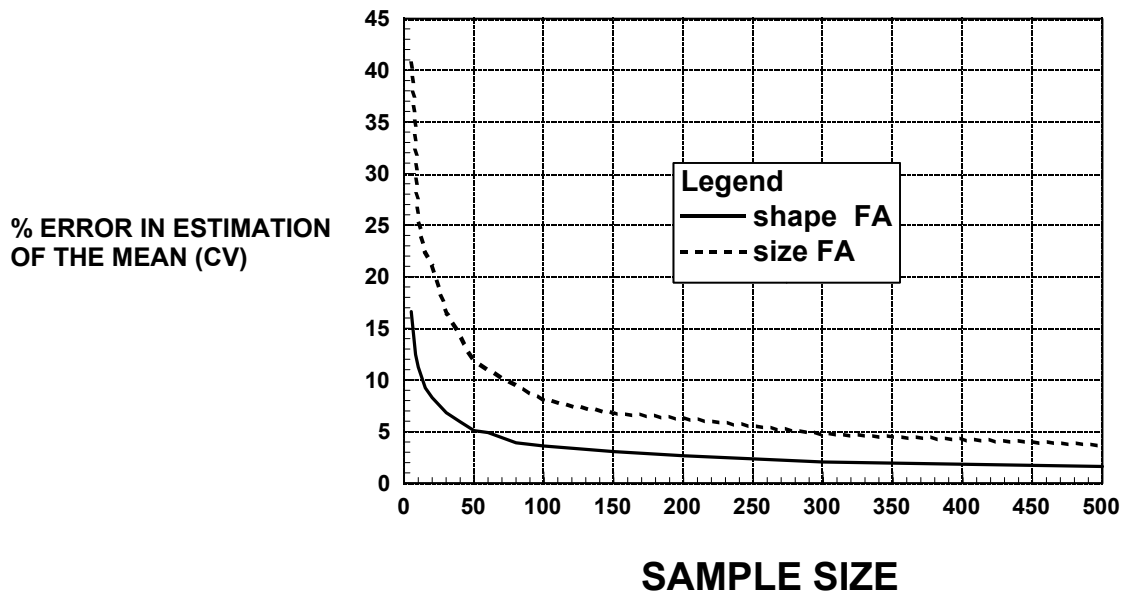


Figure 2-6. Relationship between sample size and % error for estimates of mean FA drawn from best fitting size (dashed line) and shape (solid line) distributions using 1000 draws per sample size. All runs use typical winning double Pareto lognormal parameters (shape FA $v = -3.7$, $\tau = 0.2$, $\alpha = 1000$, $\beta = 9$; for size FA $v = 1.2$, $\tau = 0.7$, $\alpha = 4.0$, $\beta = 4.0$).

Percent measurement error for shape FA was 1.41% in aphids, 1.63% in bees, and 2.42 % in flies while for size FA, it was ~4.5% in aphids, ~5% in bees, and ~6.5 % in flies. In a Procrustes ANOVA (Klingenberg and McIntyre 1998) the mean squares for the interaction term of the ANOVA ($MS_{\text{Interaction}}$) was highly significant $p < 0.001$ in all three species indicating that FA variation was significantly larger than variation in measurement error (ME). The distribution of signed ME was normal and exhibited

moderate platykurtosis for all types of FA in all species examined. Measurement error was very weakly correlated to FA in all samples ($0.01 < r^2 < 0.07$).

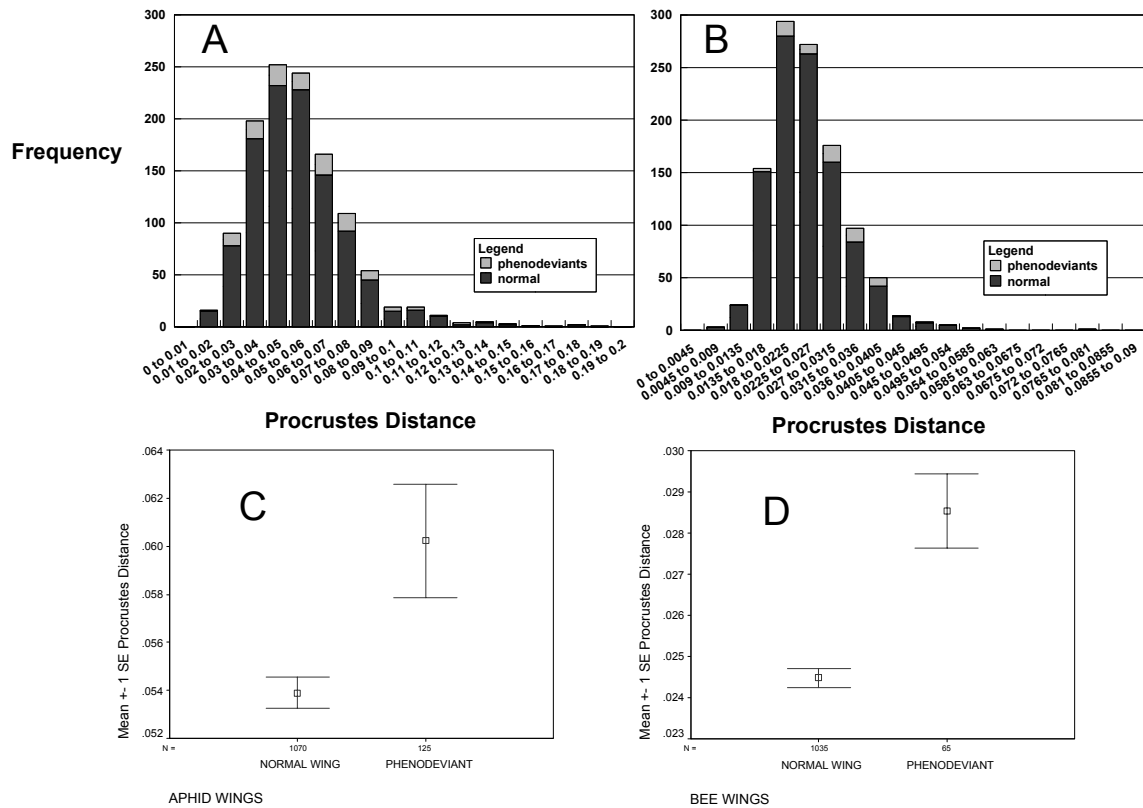


Figure 2-7. The proportion and percentage (inset) of individuals with visible developmental errors on wings (phenodeviants) are shown for cotton aphids (A) and honeybees (B) in relation to distribution of shape FA (Procrustes distance). Average FA for both normal and phenodeviant aphids (C) and honeybees (D) are also given.

Discussion

The Distribution of FA

The data demonstrate a common pattern of distribution in the FA in wing size and shape of three different species whose populations existed under very different environmental conditions (lab culture, free-living domesticated, and wild) and genetic structure (monoclonal, haplodiploid sisters, and unrelated). The similarities across the very different species and rearing conditions used in this study suggest that the

distribution of size and shape FA may have universal parameters (e.g., $\tau \approx 0.35$ for shape FA and $\tau \approx 0.7$ for size based FA). The data confirm that although size FA sometimes exhibits reasonable fit to half-normal in the upper tail, and shape FA is reasonably well fit by lognormal distributions, large datasets of FA in both size and shape are always best described by a double Pareto lognormal distribution (DPLN) or one of its limiting forms, LPLN and RPLN. Multivariate shape FA demonstrates narrow distribution with a large right tail, including the top few percent of the most extremely asymmetric individuals, that is best fit by DPLN or RPLN. Both univariate and multivariate size FA exhibit a considerably broader distribution with moderate leptokurtosis that is best fit by DPLN or LPLN. The data suggest that the DPLN distribution and its limiting forms are generally the most appropriate models for the distribution of FA regardless of method of measurement.

Evidence that distribution of FA closely follows DPLN, a continuous mixture model, and appearance of phenodeviance across nearly the entire range of data suggested that developmental errors may be caused by a similar process across the entire distribution of FA in a population. In other words, variation in FA may have a single cause in most of the data. Although phenodeviance is significantly related to increased levels of FA and is more prevalent in the right tail region of the shape FA distribution, it does not appear associated exclusively with the right tail, as a threshold model for high FA might predict. The very poor fits to all variations on the discrete mixture model also suggest a lack of distinct processes creating extreme FA in the three datasets. However, I caution that use of maximum likelihood methods to fit data to discrete mixtures is often technically challenging. I found no block effects (e.g., no differences in FA levels

between long-legged fly samples collected on different weeks or aphid samples collected from different pots or growth chambers), so it appears there is no obvious sample heterogeneity that could result in a discrete mixture. With the usual caveats about inferring process from pattern, I do not find obvious thresholds in the distribution of asymmetries at the population level that would suggest threshold effects at a genetic or molecular level. Lastly, based on the appearance of only one phenodeviant among our wild trapped long-legged fly population (as opposed to many in the bee and lab reared aphid populations), I speculate that mortality related to phenodeviance (and perhaps high FA) in wing morphology may be relaxed in lab culture and domestication. But this could be confounded by other differences between the three datasets including genetic redundancy and species differences. Further comparisons among populations of single species under different conditions would be needed to test this idea.

Sample Size and the Estimation of Mean FA

In random sampling under DPLN, we found that broad distribution effects due to the shape parameter were minimal in their effect of slowing convergence to the population mean in multivariate shape-based FA ($\tau \approx 0.35$ for all three datasets). However, these effects are considerable for univariate and multivariate size-based FA (where $\tau \approx 0.70$). The effects of scaling in the tails of the distribution, which cause divergence from the mean, appear to have little effect in the right tail of the distribution of shape-based FA. However, larger effects in the tails of the size FA create more individuals with very low and very high asymmetry than expected under the assumption of normality. The point estimates of the scaling exponents for size FA are close to the range where very extreme values may be sampled under the distribution tails (if $\alpha < 3$ or $\beta < 3$), greatly affecting confidence in the estimate of mean FA. With a sample size of 50

and the best fitting DPLN parameters typical for asymmetry in multivariate shape, we found that the coefficient of variation for mean FA is about 5%, whereas size-based mean FA fluctuates about 13% from sample to sample. At a sample size of 100, these coefficients of variation are 3.2% and 7.5% respectively. Unless experimental treatment effects in most FA studies are larger than this, which is unlikely in studies using size-based measures of FA of more canalized traits, statistical power and repeatability will be low. Given the sample size range of most previous studies ($n = 30-100$) and their tendency to favor size-based measurement methods, our results suggest that many past FA studies may be under-sampled. Furthermore, it is also likely that given the small sample sizes in many FA studies, particularly involving vertebrates where $n < 50$, the tail regions of natural FA distributions are often severely under sampled and sometimes truncated by the removal of outliers. These factors may artificially cause non-normal distributions to appear normal, also potentially resulting in inaccurate estimation of mean FA.

The Basis of Fluctuating Asymmetry

The surprisingly good fit of FA distributions to the DPLN model in our study suggests that the physical basis of FA may be created by the combination of random effects in geometrically expanding populations of cells on either side of the axis of symmetry (i.e., geometric Brownian motion). Studies in the *Drosophila* wing indicate that cell lines generally compete to fill a prescribed space during development with more rapidly dividing lines out-competing weaker ones (Day and Lawrence 2000). Because regulation of the growth of such cell populations involves either nutrients and/or signaling substances that stop the cell cycle when exhausted, it is likely that the distribution of numbers of cells present at the completion of growth follows an

exponential distribution. Reed and Jorgensen (2004) demonstrate that when a population of repeated geometric random walks is “killed” at such a constant rate, the DPLN distribution is the natural result. There are many other examples of growth processes in econometrics and physics where random proportional change combined with random stopping/observation create size distributions of the kind described here (Reed 2001; Kozubowski and Podgorski 2002). In the future, when applying this model to instability during biological growth, it would be very interesting to investigate how genetic and environmental stress might affect the parameters of this model. If scaling effects are found to vary with stress, then leptokurtosis may potentially be a better candidate signal of developmental instability than increased mean FA.

Conclusion

Although size-based FA distributions can sometimes appear to fit normal distributions reasonably well as previous definitions of FA suppose, I demonstrate that three large empirical datasets all support a new statistical model for the distribution of FA (the double Pareto lognormal distribution), which potentially exhibits power-law scaling in the tail regions and leading to uncertain estimation of true population mean at sample sizes reported by most FA studies. The assumption of normality fails every time candidate models are compared on large datasets. Failure of this assumption in many datasets may have been a major source of discontinuity in results of past FA studies. Future work should attempt to collect larger sample/treatment sizes ($n \approx 500$) unless the magnitude of treatment effects on FA (and thus the statistical power of comparisons) is very large. Our results demonstrate that multivariate shape-based methods (Klingenberg and McIntyre 1998) result in more repeatable estimates of mean FA than either multivariate or univariate size-based methods. I would also recommend that

methodology be re-examined even in large sample studies of FA. For example, because *Drosophila* are usually reared in many replicates of small tubes with less than 50 larvae per tube, many large studies may still be compromised by individual sizes of replicate samples. I also suggest that authors of past meta-analyses and reviews of FA literature reassess their conclusions after excluding studies in which under-sampling is found to be problematic. Careful attention to distributional and sampling issues in FA studies has the potential both to mitigate problems with repeatability and possibly to suggest some of the underlying mechanisms driving variation in FA among individuals, populations, and species.

CHAPTER 3

INBREEDING REDUCES POWER-LAW SCALING IN THE DISTRIBUTION OF FLUCTUATING ASYMMETRY: AN EXPLANATION OF THE BASIS OF DEVELOPMENTAL INSTABILITY

Introduction

Fluctuating asymmetry (FA) is the average difference in size or shape of paired or bilaterally symmetric morphological trait sampled across a population. The study of FA, thought to be a measure of developmental instability, has a controversial history. Fluctuating asymmetry is hypothesized by some to universally represent a population's response to environmental and/or genetic stress (Parsons 1992, Clarke 1993, Graham 1992). It is also generally accepted that FA may be co-opted as an indicator or even a signal of individual genetic buffering capacity to environmental stress (Moller 1990, Moller and Pomiankowski 1993). Recent literature reviews reveal that these conclusions are perhaps premature and analyses of individual studies often demonstrate conflicting results (Lens 2002, Bjorksten 2000). Babbitt et al. (2006) demonstrate that this conflict may be caused by under-sampling due to a false assumption that FA always exhibits a normal distribution. Also, FA may be responding to experimental treatment in a complex and as yet unpredictable fashion. Until the basis of FA is better understood, general interpretation of FA studies remains difficult.

What is the Basis of FA?

Earlier studies of sexual selection and FA conclude that FA is ultimately a result of strong selection against the regulation of the development of a particular morphology (e.g., morphology used in sexual display). Thus in some instances FA may increase and

therefore become a better signal and/or more honest indicator of good genes. Sexually selected traits tend to have increased FA (Moller and Swaddle 1997), however the exact mechanism by which FA increases remains unexplained (i.e., a black box). More recently, theoretical attempts have been made to explain how FA may be generated but none have been explicitly tested. Models for the phenomenological basis of FA fall into two general categories: reaction-diffusion models and diffusion-threshold models (reviewed in Klingenberg 2003). The former class of models involves the chaotic and nonlinear dynamics in the regulation or negative feedback among neighboring cells (Emlen et al. 1993) or adjacent bilateral morphology (Graham et al. 1993). The latter class of models combines morphogen diffusion and a threshold response, the parameters of which are controlled by hypothetical genes and a small amount of random developmental noise (Klingenberg and Nijhout 1999). The result of this latter class of model is that different genotypes respond differently to the same amount of noise, providing an explanation for genetic variation in FA response to the same environments.

Traditionally, models for the basis of FA assume that variation in FA arises from independent stochastic events that influence the regulation of growth through negative feedback rather than processes that may fuel or promote growth. None of these models explicitly or mathematically address the effect of stochastic behavior in cell cycling on the exponential growth curve. More recently Graham et al. (2003) makes a compelling argument that fluctuating asymmetry often results from multiplicative errors during growth. This is consistent with one particular detail about how cells behave during growth. For several decades there has been evidence that during development, cells actually compete to fill prescribed space until limiting nutrients or growth signals are

depleted (Diaz and Moreno 2005, Day and Lawrence 2000). Cell populations effectively double each generation until signaled or forced to stop. It has also been observed that in *Drosophila* wing disc development, that synchrony in cell cycling does not occur across large tissue fields but rather extends only to an average cluster of 4-8 neighboring cells regardless of the size and stage of development of the imaginal disc (Milan et al. 1995). The assumption of previous models, particularly the reaction-diffusion type, that cell populations are collectively controlling their cell cycling rates across a whole developmental compartment is probably unrealistic. Regulatory control of fluctuating asymmetry almost certainly does occur, but probably at a higher level involving multiple developmental compartments where competing cells are prevented from crossing boundaries. However, given that individual cells are behaving more or less autonomously during growth within a single developmental compartment, I suggest that variation in fluctuating asymmetry can be easily generated at this level by a process related to stochastic exponential expansion and its termination in addition to regulatory interactions that probably act at higher levels in the organism. In this paper, I explore and test simple model predictions regarding the generation of fluctuating asymmetry through multiplicative error without regulatory feedback.

Exponential Growth and Non-Normal Distribution of FA

In previous work, Babbitt et al. (2006) demonstrate that the distribution of unsigned FA best fits a lognormal distribution with scaled or power-law tails (double Pareto lognormal distribution or DPLN). This distribution can be generated by random proportional (exponential) growth (or geometric Brownian motion) that is stopped or observed randomly according to a negative exponential probability (Reed and Jorgensen 2004). I suggest that this source of power-law scaling in the tails of the FA distribution is

also the cause of leptokurtosis that is often observed empirically in the distribution of FA. Kurtosis is the value of the standardized fourth central moment. Like the other moments, (location, scale, and skewness), kurtosis is best viewed as a concept that can be formalized in multiple ways (Mosteller and Tukey 1977). Leptokurtosis is best visualized as the location and scale-free movement of probability mass from the shoulders of a symmetric distribution towards both its center and tail (Balanda and MacGillivray 1988). Both the Pareto and power-function distributions have shapes characterized by the power-law and a large tail and therefore exhibit a lack of characteristic scale. Both because kurtosis is strongly affected by tail behavior, and because leptokurtosis involves a diminishing of characteristic scale in the shape of a distribution, the concepts of scaling and kurtosis in real data can be, but are not necessarily always, inter-related.

Both in the past and very recently, leptokurtosis in the distribution of FA has been attributed to a mixture of normal FA distributions caused by a mixing of individuals, all with different genetically-based developmental buffering capacity, or in other words, different propensity for expressing FA (Gangestad and Thornhill 1999, Palmer and Strobek 2003, Van Dongen et al. 2005). Although not noted by these authors, continuous mixtures of normal distributions generate the Laplace distribution (Kotz et al. 2001, Kozubowski and Podgorski 2001) and can be distinguished from other potential candidate distributions by using appropriate model selection techniques, such as the Akaike Information Criterion technique (Burnham and Anderson 1998). Graham et al. (2003) rejects the typical explanation of leptokurtosis through the mixing of normal distributions by noting that differences in random lognormal variable can generate

leptokurtosis. Babbitt et al. (2006) also reject the explanation that leptokurtosis in the distribution of FA is caused by a mixture of normal distributions because the double Pareto-lognormal distribution, not the Laplace distribution, always appears the better fit to large samples of FA. Therefore, leptokurtosis, often observed in the distribution of FA, may not be due to a mixing process, but instead may be an artifact of scaling in the distribution tail, which provides evidence of geometric Brownian motion during exponential expansion of populations of cells.

Testing a Model for the Basis of FA

I propose that the proximate basis for variation of FA in a population of organisms is due to the random termination of stochastic geometric growth. The combination of opposing stochastic exponential functions results in the slow power-law decay that describes the shape of the distribution's tail. In this paper, I present a model for FA and through simulation, test the prediction that genetic variation in the ability to precisely terminate growth will lead to increased kurtosis and decreased scaling exponent in the upper tail of the distribution. Then, I assess the validity of this model by direct comparison to the distribution of FA within large samples of wild and inbred populations of *Drosophila*. Under the assumption that a less heterozygous population will have less variance in the termination of growth, I would predict that inbreeding should act to reduce power-law scaling effects in the distribution of FA in a population. Inbreeding should also reduce the tail weight (kurtosis) and mean FA assuming inbred individuals have lower variance in the times at which they terminate growth. I also assume that inbreeding within specific lines does not act to amplify FA due to inbreeding depression. It has been demonstrated that *Drosophila melanogaster* do not increase mean FA in response to inbreeding (Fowler and Whitlock 1994) and it is suggested that large

panmictic populations typical of *Drosophila melanogaster* may not harbor as many hidden deleterious recessive mutations as other species (Houle 1989), making them resistant to much of the typical genetic stress of inbreeding. Therefore, the absence of specific gene effects during inbreeding suggests that *Drosophila* may be a good model for investigating the validity of our model as an explanation of the natural variation occurring in population level FA.

Methods

Model Development

Simulation of geometric Brownian motion

Ordinary Brownian motion is most easily simulated by summing independent Gaussian distributed random numbers or white noise (X_i). See Figure 3-1.

$$(3.1) \quad W(X) = \sum_{i=1}^n X_i$$

which simulated in discrete steps is

$$(3.2) \quad N_t = N_{t-1} + W_{t-1}$$

where N = cell population size, t = time step and W = a random Gaussian variable.

Exponential or geometric Brownian motion, a random walk on a natural log scale, can be similarly simulated. Geometric Brownian motion is described by the stochastic differential equation

$$(3.3) \quad dY(t) = \mu Y(t)dt + \nu Y(t)dW(t)$$

or also as

$$(3.4) \quad \frac{dY(t)}{Y(t)} = \mu dt + \nu dW(t)$$

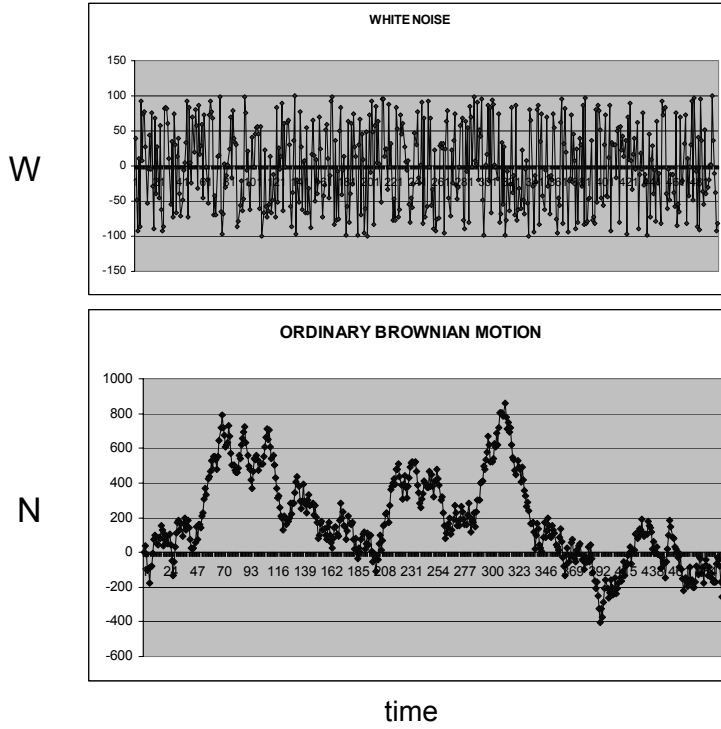


Figure 3-1. Ordinary Brownian motion (lower panel) in N simulated by summing independent uniform random variables (W) (upper panel).

where $W(t)$ is a Brownian motion (or Wiener process) and μ and ν are constants that represent drift and volatility respectively. Equation 3.3 has a lognormal analytic solution

$$(3.5) \quad Y(t) = Y(0)e^{(\mu - \nu^2/2)t + \nu W(t)}$$

A simulation of geometric Brownian motion in discrete form follows as

$$(3.6) \quad N_t = N_{t-1} + N_{t-1}W_{t-1}$$

where N = cell population size, t = time step and W = a random Gaussian variable. See Figure 3-2. Equation 3.6 is identical to the equation for multiplicative error in Graham et al. (2003). I modify equation 3.6 slightly by letting W range uniformly from 0.0 to 1.0 with $\overline{W} = 0.5$ and adding the drift constant C that allows for stochastic upward drift (at $C > 0.5$) or downward drift (at $C < 0.5$).

$$(3.7) \quad N_t = CN_{t-1} + N_{t-1}W_{t-1} = (C + W_{t-1})N_{t-1}$$

At $C = 0.5$, eqns. 3.6 and 3.7 behave identically. Geometric Brownian motion with upward drift is shown in Figure 3-3.

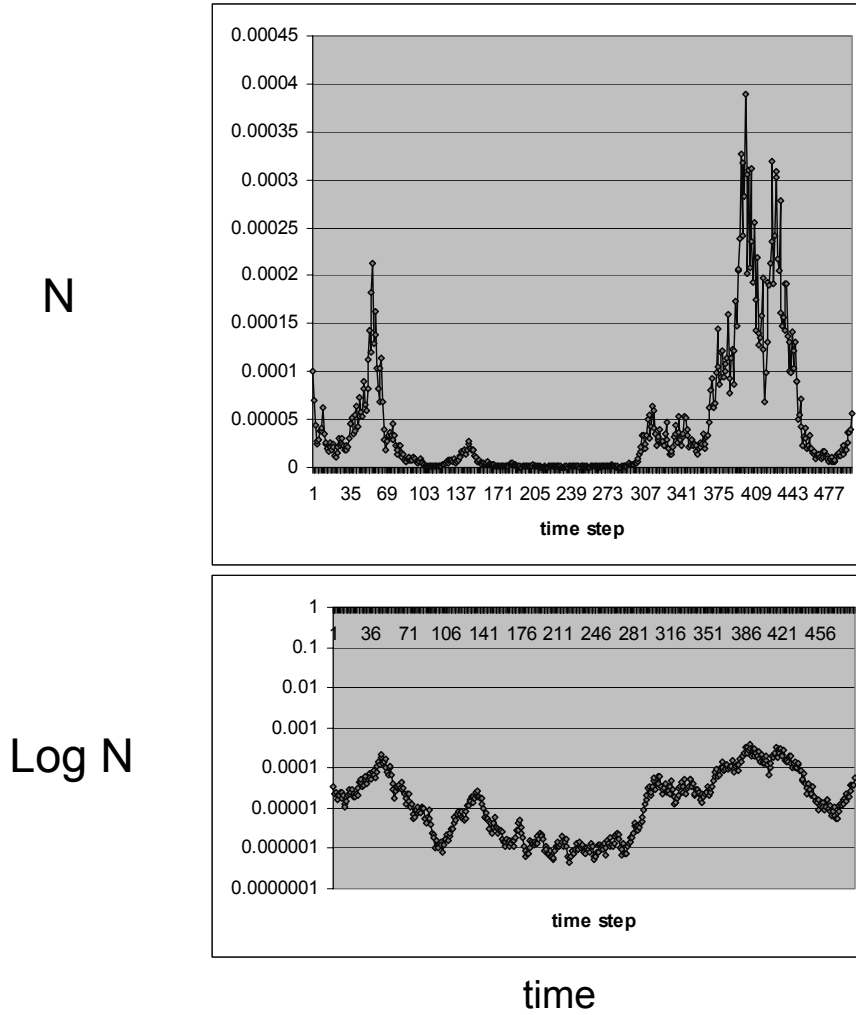


Figure 3-2. Geometric Brownian motion in N and $\log N$ simulated by multiplying independent uniform random variables. This was generated using Equation 1.5 with $C = 0.54$.

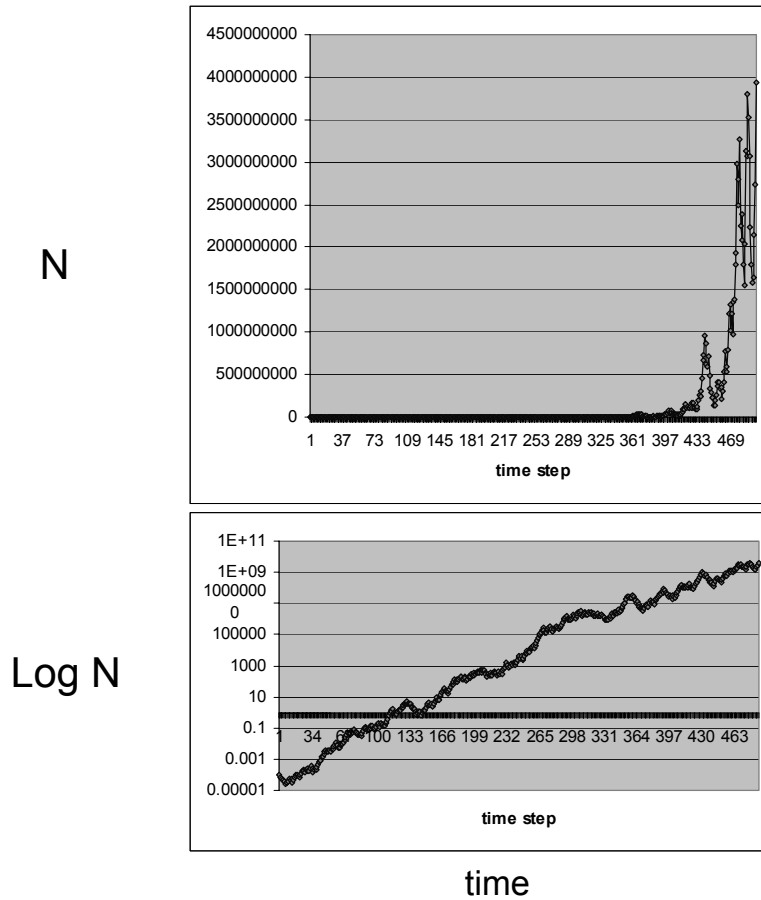


Figure 3-3. Geometric Brownian motion in N and $\log N$ with upward drift. This was generated using Equation 1.5 with $C = 0.60$.

Simulation of fluctuating asymmetry

Using the MathCad 13 (Mathsoft Engineering and Education 2005), two independent geometric random walks were performed and stopped randomly at mean time $t = 200 \text{ steps}$ with some variable normal probability. The random walks result in cell population size equal to N_t (or N_t^L and N_t^R on left and right sides respectively).

Fluctuating asymmetry (FA) was defined as the difference in size resulting from this random proportional growth on both sides of the bodies axis of symmetry plus a small degree of random uniformly distributed noise or

$$(3.8) \quad FA = N_t^L - N_t^R + rv$$

where (rv) was uniformly distributed with a range of $\pm 0.1(N_t^L - N_t^R)$. Using a MathCad-based simulation in VisSim LE, the generation of individual FA values was repeated until a sample size of 5000 was reached. The random noise (rv) has no effect on the shape of the FA distribution but fills empty bins (gaps) in distribution tails. Because rv is small in comparison to $N_t^L - N_t^R$, its effect is similar to that of measurement error (which would be normally distributed rather than uniform). Schematic representation of the simulation process for Reed and Jorgensen (2004) model and simulation of fluctuating asymmetry are shown in Figure 4 and 5. The simulation of the distribution of fluctuating asymmetry was compared at normal standard deviation of termination of growth (t) ranging from $\sigma = 0.5, 0.8, 1.2, 3$ and 7 with a drift constant of $C = 0.7$.

Inbreeding Experiment

In May 2004 in Gainesville, Florida, 320 free-living *Drosophila simulans* were collected in banana baited traps and put into a large glass jar and cultured on instant rice meal and brewer's yeast. After two generational cycles 1000 individuals were collected in alcohol. This was repeated again in June 2005 with 200 wild trapped flies.

Lines of inbred flies were created from the May 2004 wild population through eight generations of full sib crosses removing an estimated 75% of the preexisting heterozygosity (after Crow and Kimura 1970). Initially, ten individual pairs were isolated from the stock culture and mated in $\frac{1}{2}$ pint mason jars with media and capped with coffee filters. In each generation, and in each line, and to ensure that inbred lines were not accidentally lost through an inviable pairing, four pairs of F1 sibs from each cross were then mated in $\frac{1}{2}$ pint jars. Offspring from one of these four crosses were

randomly selected to set up the next generation. Of the original ten lines, only four remained viable after eight generations of full sib crossing. These remaining lines were allowed to increase to 1000+ individuals in 1 quart mason jars and then were collected for analysis in 85% ethanol. This generally took about 4 generations (8 weeks) of open breeding. One completely isogenic (balancer) line of *Drosophila melanogaster* was obtained from Dr. Marta Wayne, University of Florida and also propagated and collected.

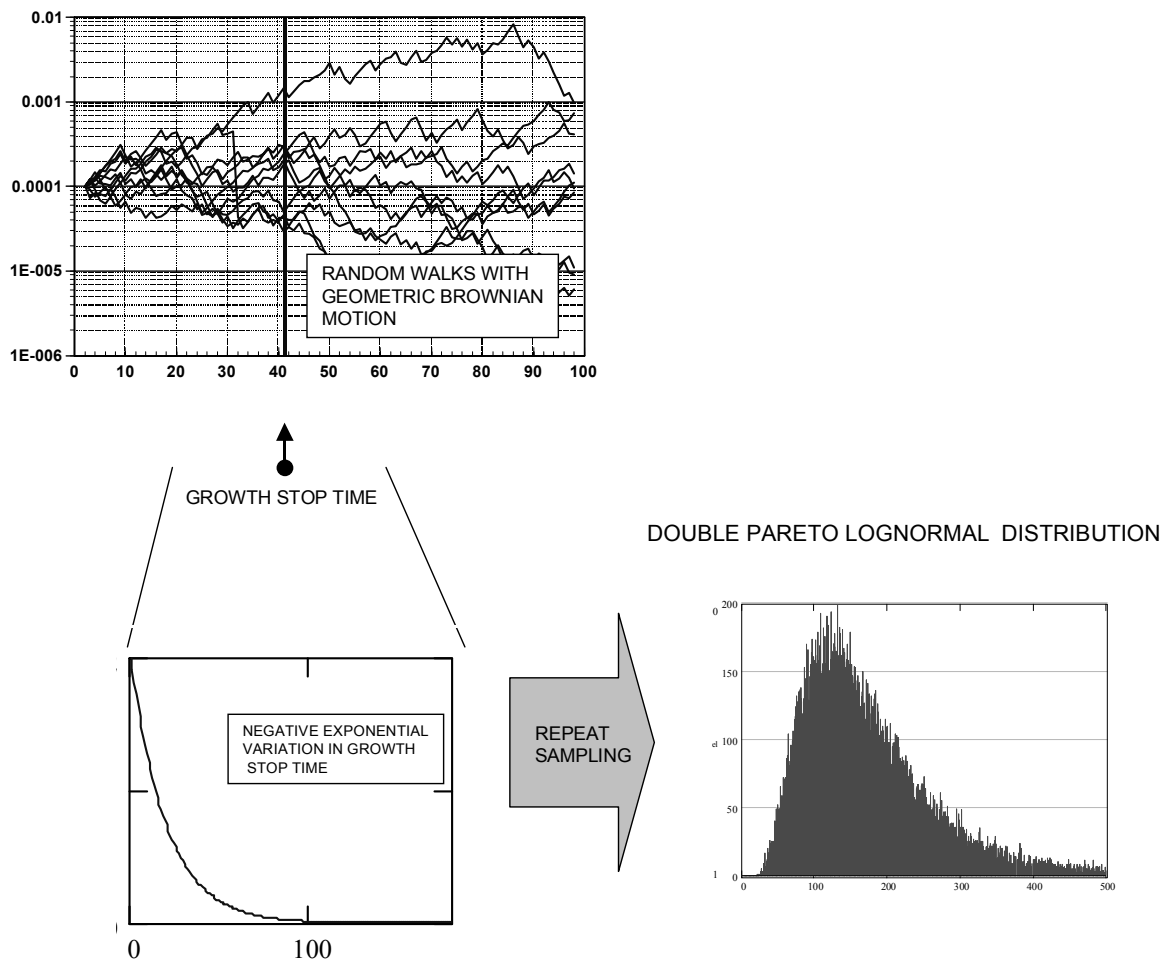


Figure 3-4. Model representation of Reed and Jorgensen's (2004) physical size distribution model. Variable negative exponentially distributed stopping Times of random proportional growth (GBM with $C = 0.5$) create double Pareto lognormal distribution of size.

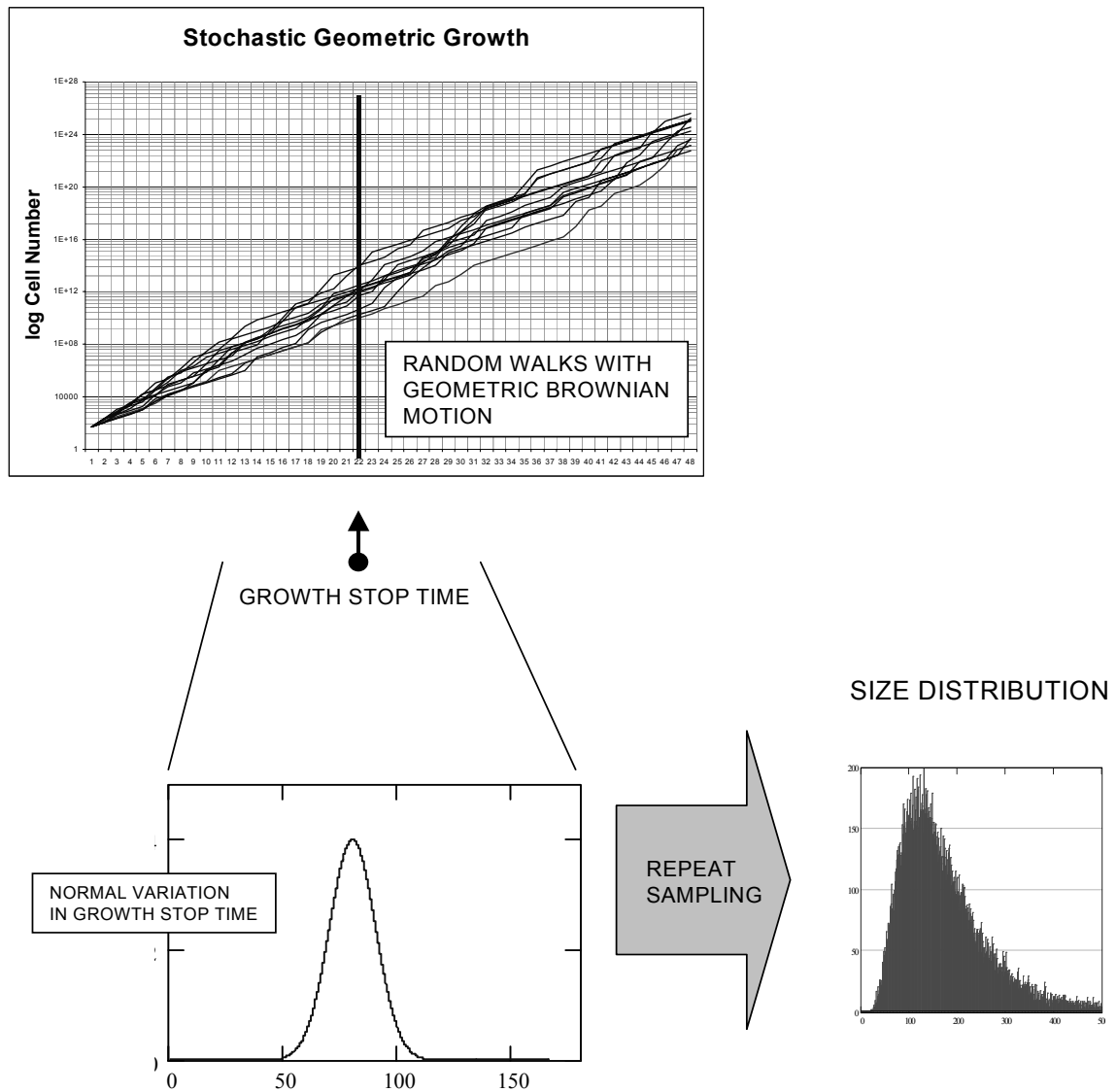


Figure 3-5. A model representation of developmental instability. Normally variable stopping times of random proportional growth (GBM with $C > 0.5$) create double Pareto lognormal distribution of size.

All flies were cultured on rice meal and yeast at 29°C with 12:12 LD cycle in environmentally controlled chambers at the Department of Entomology and Nematology at the University of Florida. Wings were collected and removed from 1000 flies from each of the two samples of wild population and four samples of inbred lines and dry mounted on microscope slides. Specimens were dried in 85% ethanol, and then pairs of

wings were dissected (in ethanol) and air-dried to the glass slides. Permount was used to attach cover slips. This technique prevented wings from floating up during mounting, which might slightly distort the landmark configuration. Dry mounts were digitally photographed. All landmarks were identified as wing vein intersections on the digital images (eight landmarks on each wing). See Appendix A for landmark locations.

Morphometric analyses

Wing vein intersections were digitized on all specimens using TPSDIG version 1.31 (Rohlf, 1999). Specimens damaged at or near any landmarks were discarded. Fluctuating asymmetry was measured in two ways on all specimens using landmark-based multivariate geometric morphometrics. A multivariate size-based FA (FA 1 in Palmer and Strobeck 2003) was calculated as absolute value of $(R - L)$ or just $R-L$ in signed FA distributions where R and L are the centroid sizes of each wing (i.e., the sum of the distances of each landmark to their combined center of mass or centroid location). In addition, a multivariate shape-based measure of FA known as the Procrustes distance was calculated as the square root of the sum of all squared Euclidean distances between each left and right landmark after two-dimensional Procrustes fitting of the data (Bookstein 1991; Klingenberg and McIntyre 1998; FA 18 in Palmer and Strobeck 2003; Smith et al. 1997). Centroid size calculation, Euclidean distance calculation and Procrustes fitting were performed using Øyvind Hammer's Paleontological Statistics program PAST version 0.98 (Hammer 2002). A sub-sample of 50 individuals from the fourth inbred line (pp4B3) was digitized five times to estimate measurement error. In these cases, measures of FA were taken as the average FA value of the five replicate measurements for each specimen. Percent measurement error was also computed as

$(ME/\text{average } FA) \times 100$ where $ME = sd(FA1, FA2, FA3, FA4, FA5)$ (as per Palmer and Strobek 2003). For assessing whether measurement error (ME) interfered significantly with FA, a Procrustes ANOVA (in Microsoft Excel) was performed on the five replications of the 50 specimen sub-sample (Klingenberg and McIntyre 1998). Any subsequent statistical analyses were performed using SPSS Base 8.0 statistical software (SPSS Inc.).

Model selection and inference

The fits of unsigned size FA to three distributional models (half-normal, lognormal, and double Pareto lognormal (DPLN)) were compared in the *Drosophila* lines, by calculating negative log likelihoods and Akaike Information Criteria (AIC) (Burnham and Anderson 1998; Hilborn and Mangel 1998). This method penalizes more complex models (those with more parameters) when selecting the best-fit distributional model for a given dataset. Best fitting parameters were obtained by maximizing the log-likelihood function for each model (Appendix B). The maximization was performed using the conjugate gradient method within unconstrained solve blocks in the program MathCAD by MathSoft Engineering and Education Inc (2001).

Results

Model Simulation

The amount of variance in termination times related directly to levels of simulated FA (i.e., low variance in termination time (t) gives low FA and vice versa). I found that not only does amount of FA increase with increased variance in (t), but so do both kurtosis and the scaling effect in the distribution tails. In Figure 3-6, normal quantile plots of signed FA are shown for different standard deviations in the normal variation of the termination of growth of geometrically expanding cell populations. The degree of the

S or sigmoidal shape in the plot indicates level of leptokurtosis. The leptokurtosis in the quantile plot is reduced greatly with a decrease in the standard deviation of the normal variation in growth termination times.

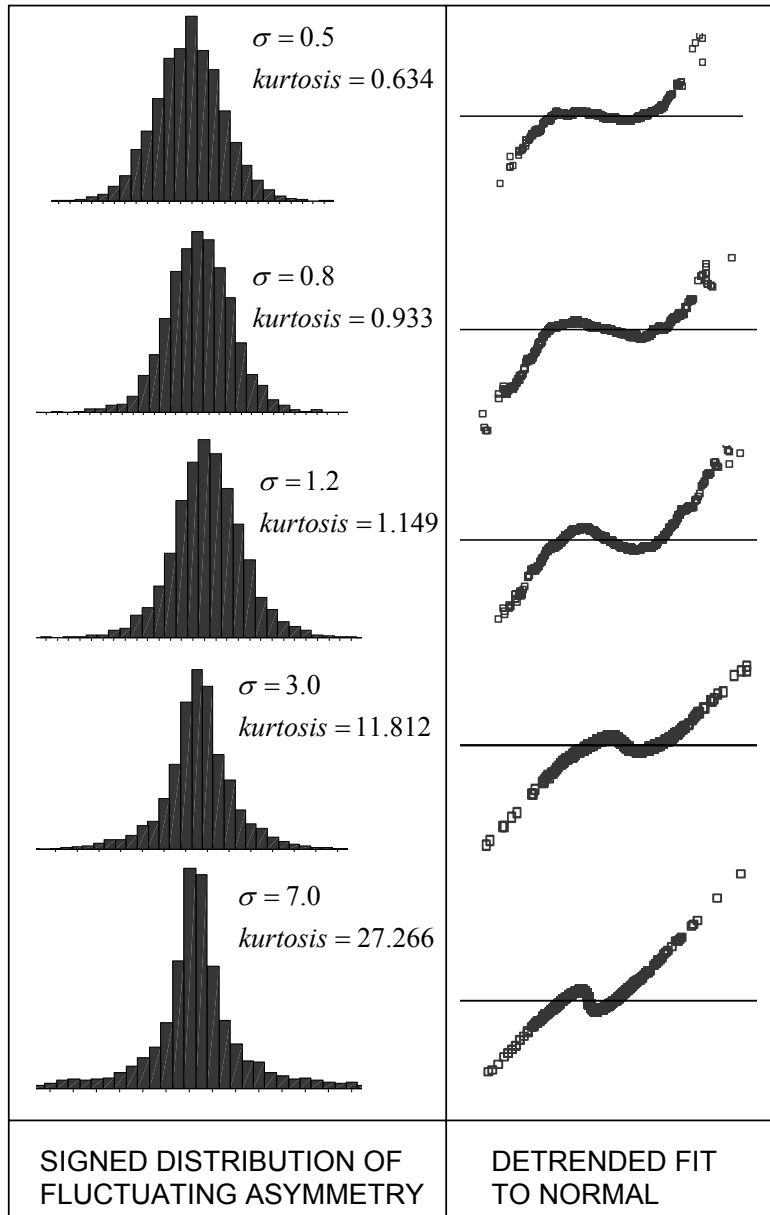


Figure 3-6. Simulated distributions of cell population size and FA for different amounts of variation in the termination of growth (variance in normally distributed growth stop time). The fit of simulated data to the normal distribution can be determined by how closely the plotted points follow the horizontal line (a good fit is horizontal).

Experimental Results

Both mean unsigned size FA and shape FA decreased with inbreeding in all lines. I also observed that the kurtosis of signed size FA and the skewness of both unsigned size and shape FA follow an identical trend. The trend was strongest in kurtosis, which decreased rapidly with inbreeding, indicating that, as predicted, changes in mean FA are influenced strongly by the shape and tail behavior of the distribution of FA (Table 3-1).

Table 3-1. Distribution parameters and model fit for multivariate FA in two wild populations and four inbred lines of *Drosophila simulans* and one isogenic line of *Drosophila melanogaster*. Model fits are Δ AIC for unsigned centroid size FA (zero is best fit, lowest number is next best fit).

| | Kurtosis (signed size FA) | Mean (unsigned size FA) | Mean (shape FA) | Scaling exponent in upper tail | Δ AIC HNORM | Δ AIC LGN | Δ AIC DPLN |
|--------------------------|---------------------------------|-------------------------------|------------------------|---|-----------------------|---------------------|----------------------|
| Wild 2004 | 28.3 ± 0.12 | 5.73 ± 0.38 | 0.0223 ± 0.0003 | 1.49 | 90.6 | 324 | 0.000 |
| Wild 2005 | 45.9 ± 0.15 | 4.68 ± 0.19 | 0.0237 ± 0.0003 | 2.87 | 66.2 | 261 | 0.000 |
| Inbred line 1 (OR18D) | 2.43 ± 0.11 | 3.27 ± 0.09 | 0.0183 ± 0.0002 | 5.09 | 0.000 | 104 | 15.5 |
| Inbred line 2(OR18D3) | 8.85 ± 0.15 | 4.24 ± 0.13 | 0.0212 ± 0.0002 | 3.10 | 11.50 | 223 | 0.000 |
| Inbred line 3 (PP4B2) | 2.90 ± 0.15 | 3.31 ± 0.09 | 0.0184 ± 0.0002 | 4.63 | 0.000 | 130 | 44.0 |
| Inbred line 4 (PP4B3) | 3.30 ± 0.15 | 3.72 ± 0.11 | 0.0213 ± 0.0003 | 5.78 | 0.000 | 228 | 79.7 |
| Isogenic (mel75) | 0.550 ± 0.11 | 3.90 ± 0.10 | 0.0201 ± 0.0002 | 9.99 | 0.000 | 84.9 | 101 |

While wild populations on the whole, demonstrated increased mean, skew and leptokurtosis of FA compared to inbred lines, significant differences between populations were found in all distributional parameters, even between each of the inbred lines (ANOVA mean size FA for all lines; $F = 27.49$, $p < 0.001$; ANOVA mean size FA for inbred lines only; $F = 14.38$, $p < 0.001$; note shape FA also show same result). Overall,

inbred lines demonstrated lower kurtosis, just slightly above that expected from a normal distribution (Table 1). They also had lower mean FA. No significant differences were found with respect to these results according to sexes of flies. In Figure 3-7, I show the distribution of FA and detrended normal quantile plots for the wild population, four inbred lines and one isogenic line respectively.

As in the simulated data, the degree of the S shape in the plot indicated level of leptokurtosis. The S shape in quantile plot is reduced greatly with inbreeding and nearly disappears in the isogenic line.

Model Selection and Inference

The comparison of candidate distributional models of FA demonstrated normalization associated with inbreeding in three of the four inbred lines (Table 3-1). In the remaining inbred line, the half-normal candidate model was a close second to the double Pareto lognormal distribution. In the wild population samples, the distribution of unsigned size-based FA was best described by the double Pareto lognormal distribution (DPLN), a lognormal distribution with scaling in both tails. In the best fitting parameters of this distribution there was no observable trend in lognormal mean or variance across wild populations and inbred lines. The scaling exponent of the lower tail (β in Reed and Jorgensen 2004) was close to one in all lines while the scaling exponent in the upper tail (α in Reed and Jorgensen 2004) increased with inbreeding (Table 3-1). Both samples of the wild population demonstrated the lowest scaling exponent in the upper tail of the distribution. The low scaling exponents here indicate divergence in variance (2004 and 2005 where $\alpha < 3$) and in the mean (2004 only where $\alpha < 2$). The inbred lines all show higher scaling exponents that are consistent with converging mean and variance.

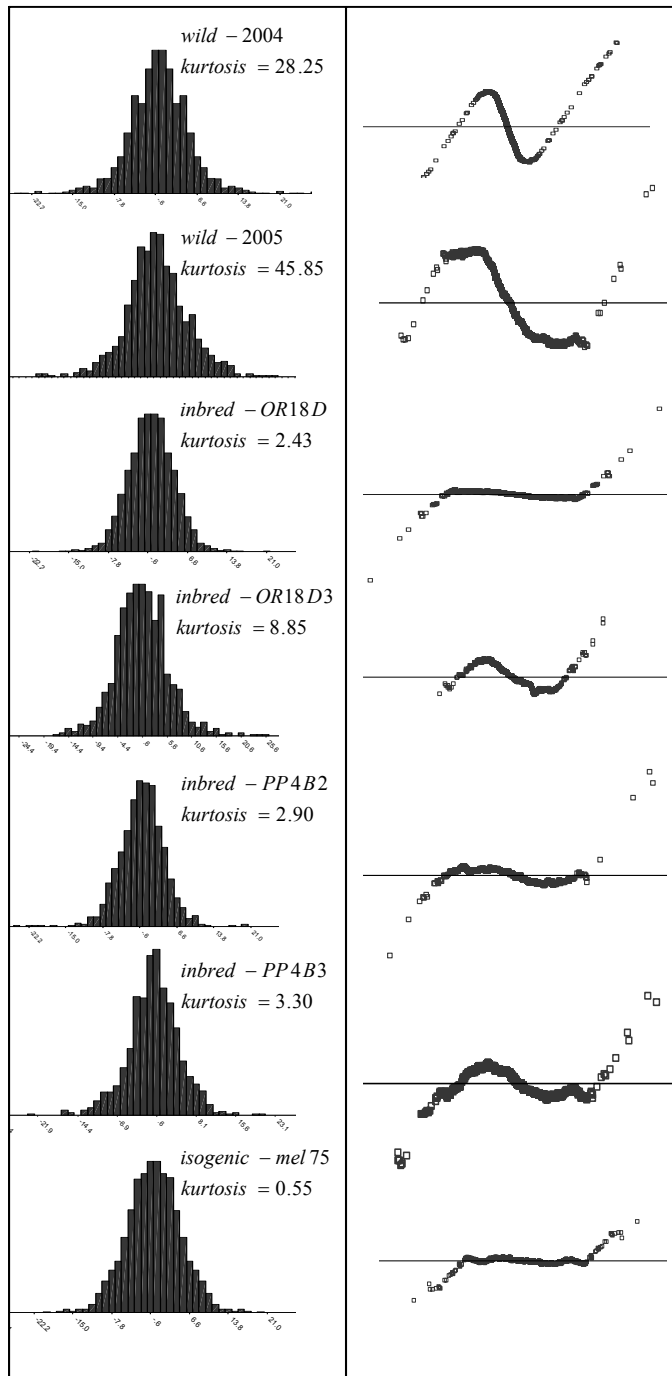


Figure 3-7. Distribution of fluctuating asymmetry and detrended fit to normal for two samples of wild population collected in Gainesville, FL in summers of 2004 and 2005 and four inbred lines of *Drosophila simulans* derived from eight generations of full-sib crossing of the wild population of 2004. Also included is one isogenic line of *Drosophila melanogaster* (mel75). All $n = 1000$. The fit of data to the normal distribution can be determined by how closely the plotted points follow the horizontal line (a good fit is horizontal).

The isogenic *Drosophila melanogaster* line demonstrated the highest scaling exponent and the most normalized distribution of unsigned FA.

Measurement error was 7.6% for shape-based FA and 13.0% for centroid size-based FA. In a Procrustes ANOVA (Klingenberg and McIntyre 1998) the mean squares for the interaction term of the ANOVA ($MS_{\text{Interaction}}$) was highly significant $p < 0.001$ indicating that FA variation was significantly larger than variation due to measurement error (ME).

Discussion

Revealing the Genetic Component of FA

While we should be cautious about inferring process from pattern, the very similar results of both the modeling and the inbreeding experiment in *Drosophila* seem to suggest the presence of a scaling component in the distribution of fluctuating asymmetry that is caused by a random multiplicative growth process as suggested previously by Graham et al. 2003. This parameter appears to change with the genetic redundancy of the population which is presumably increased by genetic drift and reduction in heterozygosity during inbreeding. Specifically, the scaling exponent(s) of the upper tail (α) of the unsigned FA distribution, or outer tails of the signed FA distribution, are increased with inbreeding, causing more rapid power-law decay in the shape of the tails. This effect also reduces kurtosis and apparently normalizes the distribution of FA in more inbred populations. This suggests that individual genetic differences in the capacity to control variance in the termination of random proportional growth (i.e., geometric Brownian motion) may be responsible for determining the shape and kurtosis of the distribution of FA. In other words, leptokurtosis (kurtosis > 3) in signed FA distribution

indicates genetic variability in the population while normality (kurtosis = 3) indicates genetic redundancy.

Because leptokurtosis is very often observed in the distribution of FA, genetic variability potentially underlies a large proportion of the variability observed in the FA of a given population. Observed differences or changes in FA are therefore not only a response of development to environmental stress, but clearly also can reflect inherent differences in the genetic redundancy of populations. The significantly different levels of mean FA among the inbred lines in this study, presumably caused by the random fixation of certain alleles, also suggests that there is a strong genetic component to the ability to buffer development against random noise. It is assumed that the differences observed in FA between wild trapped and inbred populations in this study do not indicate an effect of inbreeding depression in the study for two reasons. First, the four inbred lines analyzed in this study were vigorous in culture so the fixation of random alleles was probably not deleterious. Second, and more important, inbreeding reduced FA rather than increasing it as would have been expected under genetic stress.

It is also important to note that kurtosis is potentially a much stronger indicator of FA than the distribution mean. The low scaling exponents found in the non-normal distributions of FA in the wild populations of *Drosophila simulans* are capable of slowing and perhaps even stopping, the convergence on mean FA with increased sample size. Because kurtosis is a fourth order moment, estimating it accurately also requires larger sample sizes. However, if kurtosis can be demonstrated to respond as strongly to environmental stress as it does here to inbreeding, its potential strength as a signal of FA may allow new interpretation of past studies of FA without the collection of more data.

This may help resolve some of the current debate regarding FA as a universal indicator of environmental health and as a potential sexual signal in “good genes” models of sexual selection.

Limitations of the Model

There are certain aspects of the model presented here that may be oversimplifications of the real developmental process. First of all, this model assumes developmental instability is generated left-right growing tissue fields with no regulatory feedback or control other than when growth is stopped. It is very likely that left-right regulation is able to occur at higher levels of organization (e.g., across multiple developmental compartments) even though there is no evidence of regulated cell cycling rates beyond the distance of 6-8 cells on average within any given developmental compartment (Milan et al. 1995). Therefore this model explains how fluctuating asymmetry is generated, not how it is regulated. Second, this model only considers cell proliferation as influencing size. It is known that both cell size and programmed cell death, or apoptosis, are also important in regulating body size (Raff 1992, Conlin and Raff 1999). Both of these may play a more prominent role in vertebrate development, than they do in insect wings, where apparently growth is terminated during its exponential phase. Nevertheless, this simple model seems to replicate very well, certain behavioral aspects of the distribution of fluctuating asymmetry in the insect wing.

The Sources of Scaling

The basic process generating power-law scaling effects illustrated here (Reed 2001) offers an alternative perspective to the often narrow explanations of power-laws caused by self-organized criticality in the interactions among system components (Gisiger 2000). The power law that results from self-organized criticality is created from the multiplicity

of interaction paths in the network. As the distance between two interacting objects is increased in a network or multidimensional lattice, the number of potential interaction pathways increases exponentially, while the correlation between such paths decreases exponentially (Stanley 1995). These opposing exponential relationships create the power law scaling observed in simulations of self-organized critical systems. While there is no such “interaction” in our model, there is a power-law generated by opposing exponential functions. The constant degree of change represented by the power law in both the statistical physics of critical systems and the mathematics of both Reed and Jorgensen’s process and the model given here is the result of the combined battle between both the exponentially increasing and decreasing rates of change (Reed 2001). While the natural processes are quite different, the underlying mathematical behavior is very similar.

Potential Application to Cancer Screening

Just as changes in the shape of the distribution of fluctuating asymmetry is normalized across a population of genetically redundant individuals, genetic redundancy in a population of cells may also help maintain normal cell size and appearance. The loss of genetic redundancy in a tissue is a hallmark of cancer. The abnormal gene expression and consequent genetic instability that characterizes cancerous tissue often results in asymmetric morphology in cells, tissues and tissue borders. Baish and Jain (2000) review the many studies connecting fractal (scale free) geometry to the morphology of cancer. Cancer cells also are typically pleomorphic or more variable in size and shape than normal cells and this pleomorphism is associated with intercellular differences in the amount of genetic material (Ruddon 1995). Frigyesyi et al. (2003) have demonstrated a power-law distribution of chromosomal aberrations in cancer. Currently the type of distributional shape of the pleomorphic variability in cell size is not known, or at least not

published. However, Mendes et al. (2001) demonstrated that cluster size distributions of HN-5 (cancer) cell aggregates in culture followed a power-law scaled distribution. Furthermore these authors also demonstrated that in MDCK (normal) cells and Hep-2 (cancer) cells, cluster size distributions transitioned from short-tailed exponential distributions to long-tailed power-law distributions over time. The transition is irreversible and is likely an adaptive response to high density and long permanence in culture due to changes in either control of replication or perhaps cell signaling. Taken collectively, these studies may suggest that scaling at higher levels of biological organization observed in cancer is due to increased relative differences in length of cell cycling rates of highly pleomorphic cell populations that have relatively larger intercellular differences in amount of genetic material. The stochastic growth model I have proposed as the basis for higher variability in population level developmental instability or FA may also provide a possible explanation for higher variability in the cell sizes of cancerous tissue. If genetic redundancy in growing tissue has the same distributional effect as genetic redundancy in populations of organisms and tends to normalize the observed statistical distribution, then one might predict that the genetic instability of cancerous tissue would create a scaling effect that causes pleomorphy in cells and scaling in cell cluster aggregations. Statistical comparison of cell and cell cluster size distributions in normal and cancerous tissues may provide a useful and general screening technique for detecting when genetic redundancy is compromised by cancer in normal tissues.

Conclusion

Until now, the basis of fluctuating asymmetry has been addressed only with abstract models of hypothetical cell signaling, or elsewhere, at the level of selection

working on the organism with potential mechanism remaining in the black box.

However, fluctuating asymmetry must first and foremost be envisioned as a stochastic process occurring during tissue growth, or in other words, occurring in an exponentially expanding population of cells. As demonstrated in the model presented here, this expansion process can be represented by stochastic proportional (geometric) growth that is terminated or observed randomly over time. These results imply that the fluctuating asymmetry observed in populations is not only related to potential environmental stressors, but also to a large degree, the underlying genetic variability in those molecular processes that control the termination of growth. Therefore, fluctuating asymmetry responses to stress may be hard to interpret without controlling for genetic redundancy in the population. Both the simulation and experimental results suggest that measures of distributional shape like kurtosis, scaling exponent and tail weight may actually be a strong signal of variability in the underlying process that causes developmental instability. Therefore the kurtosis parameter of the fluctuating asymmetry distribution may provide more information about fluctuating asymmetry response than does a populations' average or mean fluctuating asymmetry. This may provide a novel method by which to resolve conflicts in previous under-sampled research without the collection of more data.

CHAPTER 4
TEMPERATURE RESPONSE OF FLUCTUATING ASYMMETRY TO IN AN APHID
CLONE: A PROPOSAL FOR DETECTING SEXUAL SELECTION ON
DEVELOPMENTAL INSTABILITY

Introduction

Developmental instability is a potentially maladaptive component of individual phenotypic variation with some unknown basis in both gene and environment (Møller and Swaddle 1997, Fuller and Houle 2003). Developmental instability is most often measured by the manifestation of fluctuating asymmetry (FA), the right minus left side difference in size or shape in a single trait across the population (Palmer and Strobeck 1986, 2003; Parsons 1992, Klingenberg and McIntyre 1998). Because FA is thought to indicate stress during development, the primary interest in the study of FA has been its potential utility as an indicator of good genes in mate choice (Møller 1990, Møller and Pomiankowski 1993) or its utility as a general bioindicator of environmental health (Parsons 1992).

The Genetic Basis of FA

For FA to become a sexually selected trait, it must be assumed that it has a significant genetic basis, and can therefore evolve (Møller 1990, Møller and Pomiankowski 1993). However, researchers who use FA as a bioindicator of environmental health often assume that FA is a phenotypic response that is mostly environmental in origin (Parsons 1992, Lens et al. 2002). Studies of the heritability of FA seem to indicate low heritability for FA exists (Whitlock and Fowler 1997, Gangestad

and Thornhill 1999). However, because FA is essentially a variance that is often measured with only two data points per individual, FA may have a stronger but less easily detectable genetic basis (Whitlock 1996, Fuller and Houle 2003). Additive genetic variation in FA in most studies has been found to be minimal, but several quantitative trait loci studies suggest significant dominance and character specific epistatic influences on FA (Leamy 2003, Leamy and Klingenberg 2005). Babbitt (chapter 3) has demonstrated that a population's genetic variability affects the distributional shape of FA. So while studies investigating mean FA may be inconclusive, changes in the population's distributional shape seem to indicate potential genetic influence on FA. However, no studies have observed FA in a clonal organism for the express purpose of assessing developmental instability that is purely environmental (i.e., non-genetic) in its origin (i.e., developmental noise).

The Environmental Basis of FA

It has long been assumed that FA is the result of some level of genetically-based buffering of additive independent molecular noise during development. Because of the difference in scale between the size of molecules and growing cells it would be unlikely that molecular noise would comprise an important source of variation in functioning cells. However, Leamy and Klingenberg (2005) rationalize that molecular noise could only scale to the level of tissue when developmentally important molecules exist in very small quantity (e.g., DNA or protein) and therefore FA may represent a stochastic component of gene expression. This is somewhat similar in spirit to the Emlen et al. (1993) explanation of FA that invokes non-linear dynamics of signaling and supply that may also occur during growth. Here FA is thought to be the result of the scaling up of

compounding temporal asymmetries in signaling between cells during growth. In this model, hypothetical levels of signaling compounds (morphogens) and or growth precursors used in the construction of cells vary randomly over time. When growth suffers less interruption, thus when it occurs faster, there is also less complexity (or fractal dimension) in the dynamics of signaling and supply. Graham et al. (1993) suggest that nonlinear dynamics of hormonal signaling across the whole body may also play a similarly important role in the manifestation of FA. However, while the levels of FA are certainly influenced by the regulation of the growth process, both Graham et al. (2003) and Babbitt (chapter 3) also suggest that FA levels reflect noise during cell cycling that is amplified by exponentially expanding populations of growing cells.

Although the proximate basis of FA is not well understood, its ultimate evolutionary basis, while heavily debated, is easier to understand. Møller and Pomiankowski (1993) first suggested that strong natural or sexual selection can remove regulatory steps controlling the symmetric development of certain traits (e.g., morphology used in sexual display). They suggest that with respect to these traits (and assuming that they are somehow costly to produce), individuals may vary in their ability to buffer against environmental stress and developmental noise in relation to the size of their individual energetic reserves; which are in turn often indicative of individual genetic quality. Therefore high genetic quality is associated with low FA.

Most existing proximate or growth mechanical explanations of FA assume that rapid growth is less stressful in the sense that fewer interruptions of growth by various types of noise should result in lower FA (Emlen et al. 1993, Graham et al. 1993). However, ultimate evolutionary explanations of FA assume that rapid growth is

potentially more stressful because it is energetically costly and therefore rapid growth should increase the level of FA when energy supply is limiting (Møller and Pomiankowski 1993). This high FA is relative and so should be especially prominent in individuals of lower genetic quality who can least afford to pay this additional energy cost. This fundamental difference between the predictions of proximate (or mechanistic) level and ultimate evolutionary level effects of temperature on FA is shown in Figure 1. The theoretical difference in the correlation of temperature and growth rate to FA in both the presence and absence of energetic limitation could be used to potentially detect sexual selection on FA. However it first should be confirmed that FA should decrease with more rapid growth in the absence of energetic limitation to growth and genetic differences between individuals in a population. This later objective is the primary goal of this study.

Temperature and FA in and Aphid Clone

At a very basic level, entropy or noise in physical and chemical systems has a direct relationship with the physical energy present in the system. This energy is measured by temperature. Because FA is speculated to tap into biological variation that is somewhat free of direct genetic control, it may therefore respond to temperature in simple ways.

First, increased temperature may increase molecular entropy which may in turn increase developmental noise during development thereby increasing FA. Second, increased temperature may act as a cue to shorten development time (as in many aphids where higher temperature reduces both body size and development time), thereby reducing the total time in which developmental errors may occur. This should reduce

FA. A third possibility is that a species specific optimal temperature exists. If so, FA should increase while approaching both the upper and lower thermal tolerance limits of organisms.

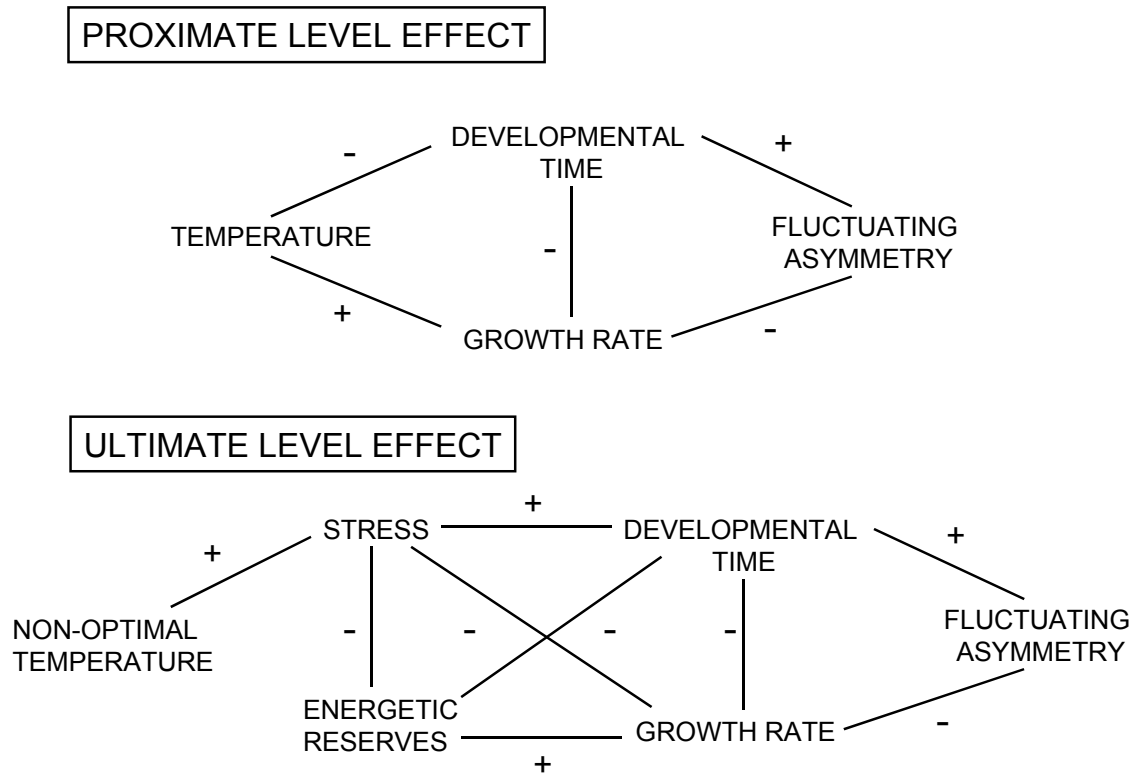


Figure 4-1. Predicted proximate and ultimate level correlations of temperature and growth rate to fluctuating asymmetry are different. Ultimate level (evolutionary) effects assume energetic limitation of individuals in the system. Proximate level (growth mechanical) effects do not. Notice that temperature and fluctuating asymmetry are negatively correlated in the proximate model while in the ultimate model they are positively correlated.

Only a few studies have directly investigated the relationship between FA and temperature. The results are conflicting. FA is either found to increase on both sides of an “optimal” temperature (Trotta et al. 2005, Zakarov and Shchepotkin 1995), to be highest at low temperature (Chapman and Goulson 2000), to simply increase with increasing temperature (Savage and Hogarth 1999, Mpho et al. 2002) or not to respond

(Hogg et al. 2001). None of these studies investigate the relationship between developmental noise (FA in a clonal line) and temperature.

The characterization of developmental noise in response to temperature was investigated in this study using the cotton aphid, *Aphis gossipyii*. These aphids reproduce parthenogenetically, are not energetically limited in their diet (because they excrete excess water and sugar as “honeydew”) and produce wings that are easily measured using multiple landmarks. They demonstrate large visible variation in body size, wing size and even wing FA. The visible levels of wing asymmetry in cotton aphids reflect levels of FA that are about four times higher than that observed in other insect wings (Babbitt et al. 2006, Babbitt in press). Because parthenogenetic aphids cannot purge deleterious mutations each generation and because Florida clones often never use sexual reproduction to produce over-wintering eggs, this remarkably high FA may be the result of Muller’s ratchet. Cotton aphids are also phenotypically plastic in response to temperature, producing smaller lighter morphs at high temperatures and larger dark morphs at low temperatures. This feature allows observation of two genetically homogeneous groups in which different gene expression patterns (causing the color morphs) exist. The central prediction is that of the proximate effect model: that in the absence of energetic limitation and genetic variation, temperature and environmentally induced FA (or developmental noise) should be negatively correlated in a more or less monotonic relationship.

Methods

In March 2003, a monoclonal population of Cotton Aphids (*Aphis gossipyii* Glover) was obtained from Dr. J.P. Michaud in Lake Alfred, Florida and was brought to

the Department of Entomology and Nematology at the University of Florida. The culture was maintained on cotton seedlings (*Gossipium*) grown at different temperatures (12.5°C, 15°C, 17°C, 19°C, 22.5°C and 25°C with $n = 677$ total or about 100+ per treatment) under artificial grow lights (14L:10D cycle). Because of potential under-sampling caused by a non-normal distribution of FA (see Babbitt et al. 2006), a second monoclonal population collected from Gainesville, FL in June 2004 was reared similarly but in much larger numbers at 12.5°C, 15°C, 17°C, 19°C, and 25°C ($n = 1677$ or about 300+ per treatment).

Development time for individual apterous cotton aphids (Lake Alfred clone) were determined on excised cotton leaf discs using the method Kersting et al. (1999). Twenty randomly selected females were placed upon twenty leaf discs (5 cm diameter) per temperature treatment. Discs were set upon wet cotton wool in petri dishes and any first instar nymphs (usually 3-5) appearing in 24 hours were then left on the discs. Development time was taken as the average number of days taken to reach adult stage and compared across temperatures. Presence of shed exoskeleton was used to determine instar stages. Cotton was wetted daily and leaf discs were changed every 5 days. Humidity was maintained at $50 \pm 5\%$.

In each temperature treatment, single clonal populations were allowed to increase on plants until crowded in order to stimulate alate (winged individuals) production. Temperature treatments above 17°C produced light colored morphs that were smaller and tended to feed on the undersides of leaves of cotton seedlings. Temperature treatments below 17°C produced larger dark morphs that tended to feed on the stems of cotton seedlings. Alatae were collected using small brushes dipped in alcohol and stored in 80%

ethanol. Wings were dissected using fine insect mounting pins and dry mounted as pairs on microscope slides. Species identification was by Dr. Susan Halbert at the State of Florida Department of Plant Industry in Gainesville.

Specimens were dried in 85% ethanol, and then pairs of wings were dissected (in ethanol) and air-dried to the glass slides while ethanol evaporated. Permount was used to attach cover slips. This technique prevented wings from floating up during mounting, which might slightly distort the landmark configuration. Dry mounts were digitally photographed. Six landmarks were identified as the two wing vein intersections and four termination points for the third subcostal. See Appendix A for landmark locations.

Wing vein intersections were digitized using TPSDIG version 1.31 (Rohlf, 1999). Specimens damaged at or near any landmarks were discarded. Fluctuating asymmetry was calculated using a multivariate geometric morphometric landmark-based method. All landmarks are shown in Appendix A. FA (FA 1 in Palmer and Strobeck 2003) was calculated as absolute value of $(R - L)$ where R and L are the centroid sizes of each wing (i.e., the sum of the distances of each landmark to their combined center of mass or centroid location). In addition, a multivariate shape-based measure of FA known as the Procrustes distance was calculated as the square root of the sum of all squared Euclidean distances between each left and right landmark after two-dimensional Procrustes fitting of the data (Bookstein 1991; Klingenberg and McIntyre 1998; FA 18 in Palmer and Strobeck 2003; Smith et al. 1997). This removed any difference due to size alone. Centroid size calculation, Euclidean distance calculation and Procrustes fitting were performed using Øyvind Hammer's Paleontological Statistics program PAST version 0.98 (Hammer 2002). Percent measurement error was computed as $(ME/average$

FA) $\times 100$ where $ME = (|FA1 - FA2| + |FA2 - FA3| + |FA1 - FA3|)/3$ in a smaller subset (200 wings each measured 3 times = $FA1$, $FA2$ and $FA3$) of the total sample. All subsequent statistical analyses were performed using SPSS Base 8.0 statistical software (SPSS Inc.). Unsigned multivariate size and shape FA as well as the kurtosis of signed FA were then compared at various temperatures using one-way ANOVA.

Results

Development time (Figure 4-2) was very similar to previously published data (Kersting et al. 1999, Xia et al. 1999) decreasing monotonically at a much steeper rate in dark morphs than in light morphs. The distributional pattern of centroid size, size FA and shape FA appear similar exhibiting right log skew distributions (Figure 4-3). Similar distributional patterns are observed within temperatures (not shown) as that observed across temperatures (Figure 4-3).

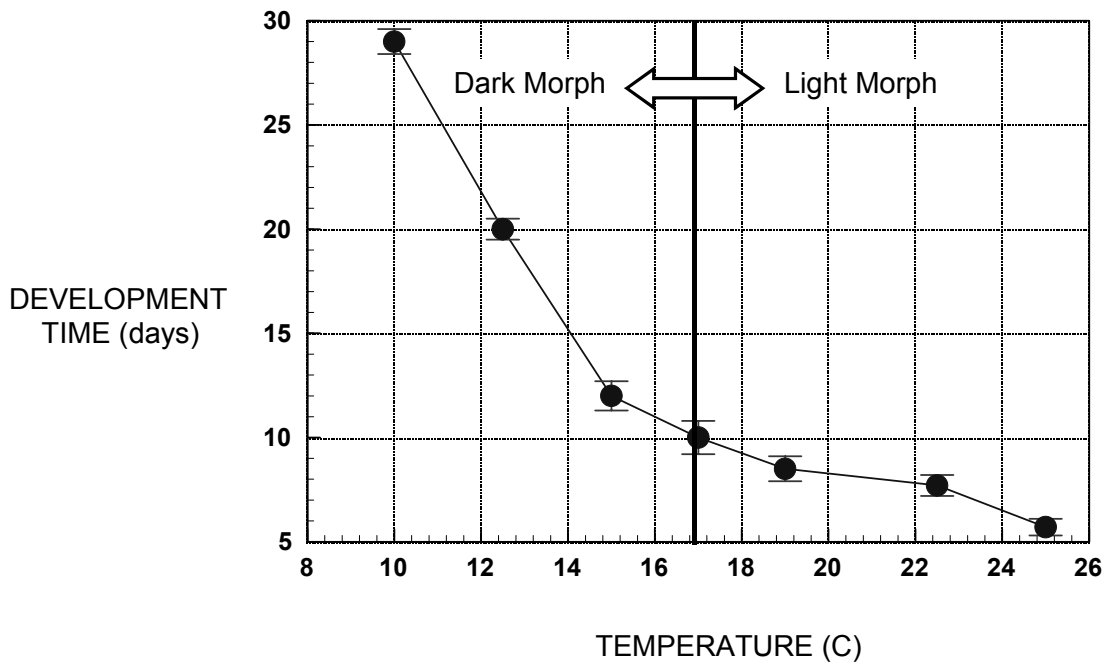
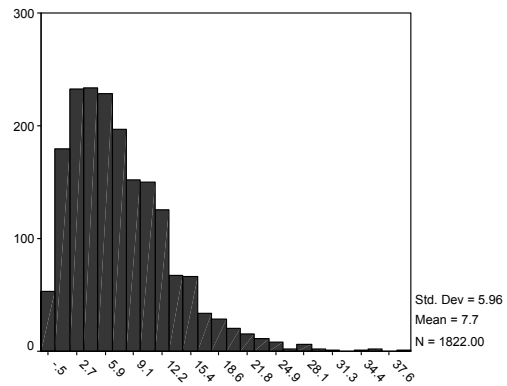
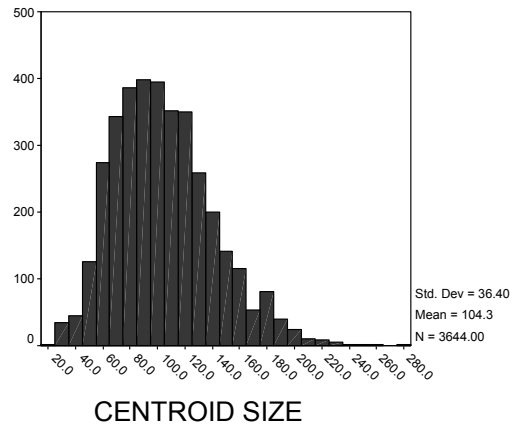
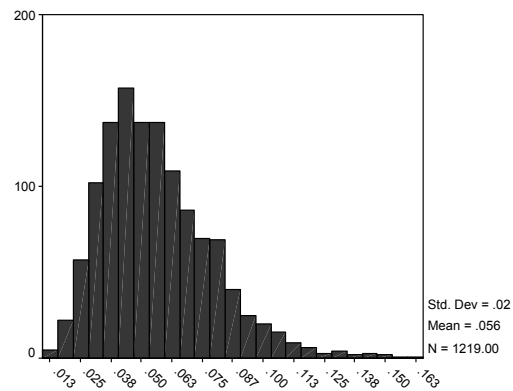


Figure 4-2. Cotton aphid mean development time ± 1 SE in days in relation to temperature ($n = 531$).

FREQUENCY



CENTROID SIZE FLUCTUATING ASYMMETRY



SHAPE FLUCTUATING ASYMMETRY

Figure 4-3. Distribution of isogenic size, size based and shape based FA in monoclonal cotton aphids grown in controlled environment at different temperatures. Distributions within each temperature treatment are similar to overall distributions shown here.

Coefficient of variation for FA was slightly higher for dark morphs (12.5 C = 92.59%, 15 C = 93.02%, 17 C = 88.95%, 19 C = 79.02%, 22.5 C = 80.00% and 25 C = 85.35%). Mean isogenic FA (both size and shape) was highly significantly different across temperatures (ANOVA $F = 6.691$, df between group = 4, df within group = 1673, $p < 0.001$) in the Gainesville FL clone (Figure 4-4) but not in the Lake Alfred clone (ANOVA $F = 1.992$, df between group = 5, df within group = 672, $p < 0.078$). This is an indication of undersampling in the Lake Alfred clone. In the Gainesville clone, mean centroid size FA (Figure 4-4A) and development time (Figure 4-2) follow a nearly identical pattern, decreasing rapidly at first then slowing with increased temperature.

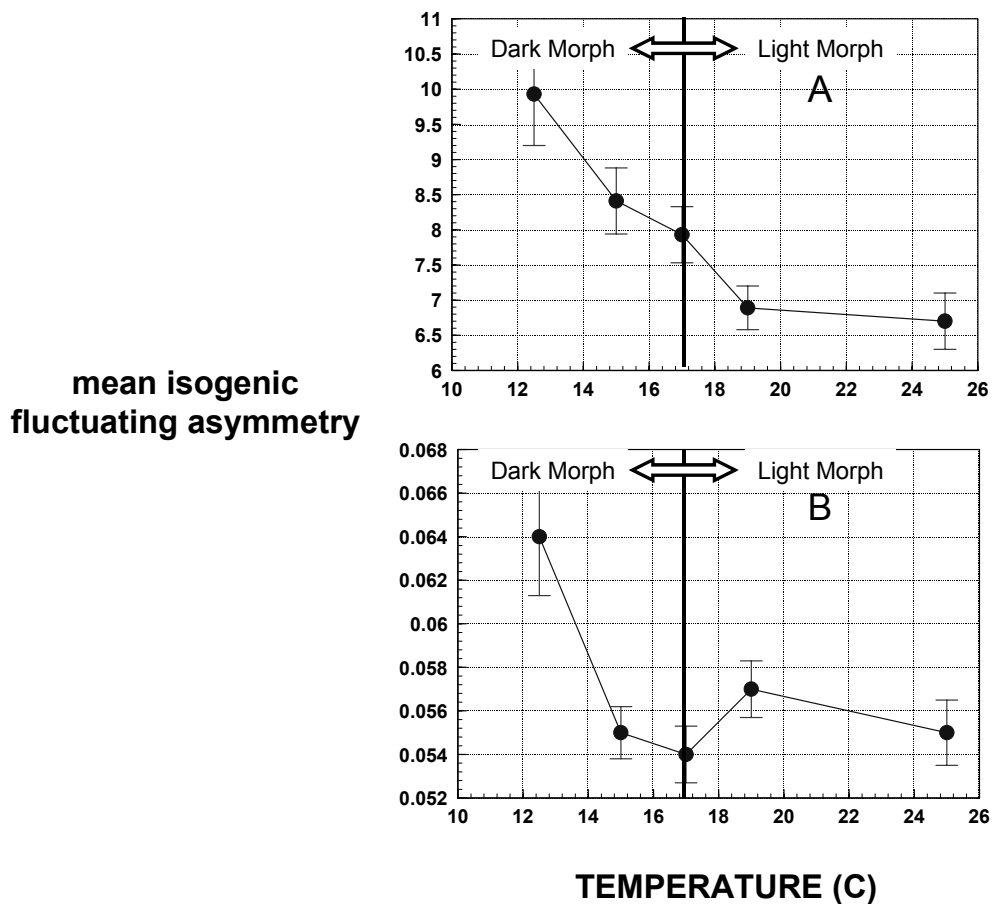


Figure 4-4. Mean isogenic FA for (A.) centroid size- based and (B.) Procrustes shape-based) in mono-clonal cotton aphids (collected in Gainesville FL) grown on isogenic cotton seedlings at different temperatures.

Mean shape FA was also significantly different across temperature classes (ANOVA $F = 4.863$, df within group = 4, df between group = 1673, $p = 0.001$) but this difference is due solely to elevated FA in the 12.5°C group (Figure 4-4B). Less than one percent of the variation in FA was due to variation in body size ($r = -0.101$ for shape FA; $r = 0.088$ for size FA). Kurtosis in the shape of the distribution of size based FA (Figure 4-5) was significantly higher in dark morphs than in light morphs ($t = -2.21$, $p = 0.027$). Within each morph (light or dark), kurtosis in the distribution of FA appears to increase with temperature slightly (Figure 4-5). Measurement error for shape FA was estimated at 2.6% (Lake Alfred clone) and 2.2% (Gainesville clone). For size FA these estimates were 6.1% (Lake Alfred) and 5.7% (Gainesville).

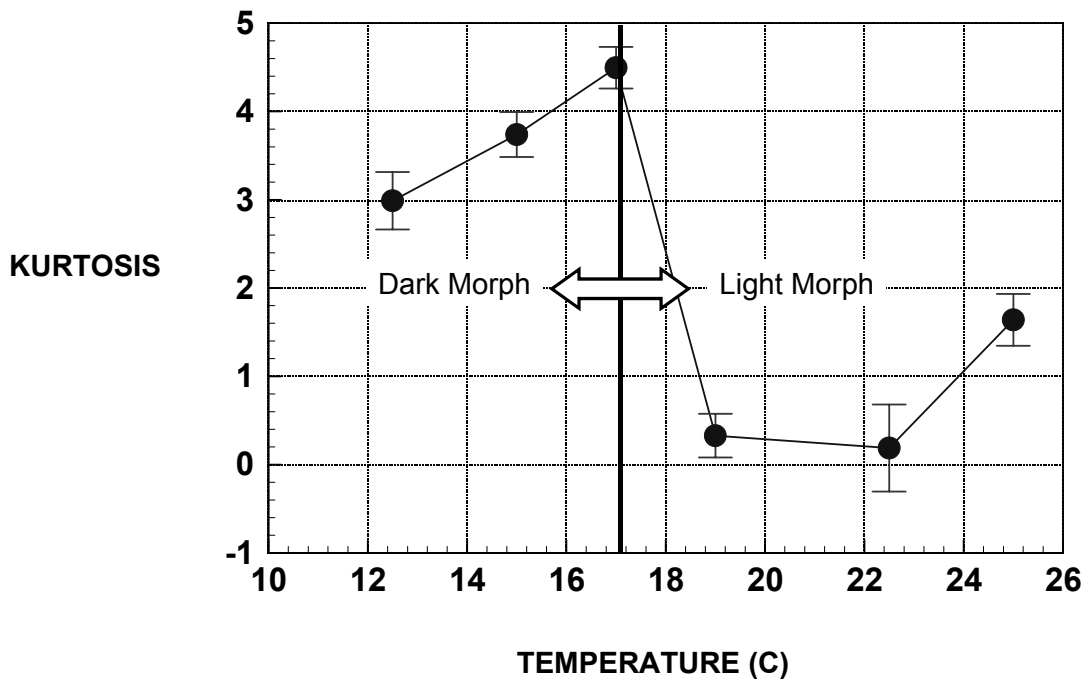


Figure 4-5. Kurtosis of size-based FA in monoclonal cotton aphids grown on isogenic cotton seedlings at different temperatures.

Discussion

It appears that the prediction of the proximate effect model holds in the case of this population of cotton aphid, which, in general, is not energetically limited and in this study, is not genetically variable. Temperature and growth rate (which are positively correlated in insects) are negatively associated with purely environmentally derived FA (i.e., developmental noise). This confirms the predictions of several proximate models of the basis of FA. Furthermore, it appears that centroid size-based FA is a simple function of development time. Because individual genetic differences in the capacity to buffer against developmental noise are, in a sense, controlled for in this study by the use of natural clones, the response of FA to temperature in this study represents a purely environmental response of FA. The fact that aphids excrete large amount of water and sugar in the form of honeydew, as well as the lack of a strong correlation between FA and size also suggests that there is no real energetic “cost” to being large in the aphids in this study. An important next step will be to compare this result to the association of growth rate to FA in genetically diverse and energetically limited sexually selected traits where the predicted association between growth rate and FA would be the opposite of this study.

It also appears that because the environmental component of size-based isogenic FA is largely a function of developmental time and temperature, dark morphs of cotton aphids, which have much longer development time than light morphs, also have significantly higher FA. The temperature trend in mean FA within both light and dark morphs, where development times are similar, is not consistent although it appears that the kurtosis of FA increases slightly with temperature within each morph.

It is very interesting that there is a strong difference in kurtosis between the two temperature morphs in this study. Previous work suggests that kurtosis is related to genetic variability in a population (Babbitt in press). The difference observed here in light of genetic homogeneity in the monoclonal aphid cultures, suggests that there may be a difference in developmental stability of light and dark aphid morphotypes that is due primarily to the differential expression of genes in each phenotype.

It is surprising that temperature trends in mean developmental noise are slightly different regarding whether a size or shape-based approach was used. In populations where individuals are genetically diverse, both size and shape-based measures of FA are often correlated to some degree (as they are here too). However, size and shape are regulated somewhat differently in that cell proliferation is mediated both extrinsically via cyclin E acting at the G1/S checkpoint of the cell cycle, predominantly affecting size, and intrinsically at via *cdc25/string* at the G2/M checkpoint, predominantly affecting pattern or shape (Day and Lawrence 2000). Extrinsic mechanisms regulate size through the insulin pathway and its associated hormones (Nijhout 2003) providing a link between size and the nutritional environment. This may explain why size FA follows development time more closely than shape FA in this study.

Size is usually less canalized than is shape and therefore more variable. While this makes the size-based measure of FA generally attractive, it has been found in previous work (Babbitt et al. 2006) that population averages of size-based FA are often so variable that they are frequently under-sampled because of the broad and often long tailed distribution of FA. Shape-based FA does not suffer as much from this problem and so its estimation is much better although it may be less indicative of environmental influences

and perhaps therefore better suited for genetic studies of FA. Because size FA has been adequately sampled in this study and because size is more heavily influenced by environmental factors like temperature, I find that size-based FA is the more interesting measure of developmental instability in this study.

In general, it is clear that developmental noise is not constant in genetically identical individuals cultured under near similar environments. The overall distribution pattern in both size and shape FA is log skewed even within temperature classes. This suggests that sampling error due solely to random noise can play a very significant role in FA studies. Furthermore, it appears that the response of FA to the environment is potentially quite strong. This suggests that FA may indeed be a responsive bioindicator, however its response will not be very generalizable in environments with fluctuation in temperature.

In conclusion, the environmental response of developmental noise to temperature in absence of genetic variability and nutrient limitation supports an important prediction of theoretical explanations of the proximate basis of FA. This prediction is that FA should decrease with growth rate (and temperature) in ectothermic organisms. Because it is only in sexually selected traits that the opposite prediction should hold, that FA should increase and not decrease with growth rate, the results presented here may offer a useful method for discriminating between FA that is under sexual selection and FA that is not.

CHAPTER 5

CONCLUDING REMARKS AND RECOMMENDATIONS

In this dissertation, I confirm some existing hypotheses concerning FA and provide a new explanatory framework that explains alteration in the distribution of fluctuating asymmetry (FA) and its subsequent effect upon mean FA. The basis of FA and the influences that shape its response to genes and the environment in populations can be suitably modeled by stochastic proportional growth in expanding populations of cells on both sides of the body that are terminated with a small degree of genetically-based random error. I model stochastic growth with geometric Brownian motion, a random walk on a log scale. And I also model error in terminating growth with a normal distribution. The resulting distribution of FA is a lognormal distribution characterized by power-law scaled tails. Because under a power-law distribution, increased sample size increases the chance of sampling rare events under these long tails, convergence to the mean is potentially slowed or even stopped depending on the scaling exponents of the power-law describing the tails. I demonstrated that the effect of reduced convergence to the mean is substantial and has probably caused much of the previous work on FA to be under-sampled (Chapter 1). I have also demonstrated that the scaling effect in the distribution of FA is directly related to genetic variation in the population. Therefore a low scaling exponent and also high kurtosis is associated with a large degree of genetic variation between individuals in their ability to precisely terminate the growth process (Chapter 2). I also demonstrate that when genetic differences do not exist (where FA is comprised of only developmental noise) and when development is not limited

energetically, such as in a parthenogenetic aphid clone, FA depends upon developmental time (Chapter 3).

How Many Samples Are Enough?

The answer to this clearly depends upon whether researchers chose to study FA in size or FA in shape. The required sample size depends upon the distributional type and parameters of the distribution of FA. As previously discussed, FA distributions differ depending upon whether FA is based on size or shape differences between sides. As demonstrated in chapter 1, multivariate measures of FA based upon shape, such as Procrustes Distances, tend to have distributional parameters that allow convergence to the mean that is about five times more rapid than either univariate or multivariate measures of FA based upon size (Euclidian distance or centroid size). While this information might seem to favor a shape-based approach, there are some other very important considerations given below. In the end, sample size must be independently evaluated in each study depending on the magnitude of asymmetry that one wishes to detect between treatments or populations. As a general rule, if shape FA is used, 100-200 samples may suffice, but if size FA is used then many hundreds or even a thousand samples may be required to detect a similar magnitude difference.

What Measure of FA is best?

The handicap of sampling requirements of size-based FA aside, it appears that measures of the distributional shape of FA, like kurtosis, scaling exponent in the upper tail and skewness are strongly related to similar but smaller changes in mean size FA (chapter 2). Because size FA is most commonly used in past studies of FA, these measures of distribution shape might allow clearer conclusions to be drawn from literature reviews and meta-analyses as well as individual studies of FA where the

collection of more data is not possible. My work linking shape of the FA distribution to the genetic variability of the population will require that future studies of FA which are focused on the environmental component of FA be controlled for genetic differences between populations. Where FA is sought as a potential bioindicator of environmental stress, the potentially differing genetic structure of populations will need to be considered in order to make meaningful conclusions about levels of FA. Additionally, because in the absence of genetic variation in monoclonal aphids, size FA is directly related to the total developmental times of individuals (chapter 3), it may a better choice than shape FA for studies of environmental influences on FA.

In most organisms, body size is less canalized than body shape. Body size is highly polygenic and depends upon many environmentally linked character traits. However body shape or patterning is determined by a sequential progression of the activity of far fewer genes. Body size is also regulated at a different checkpoint during the cell cycle than is body pattern formation or shape (Day and Lawrence 2000). Patterning or shape is regulated at G2/M checkpoint while size is regulated at G1/S checkpoint. The latter checkpoint is associated with the insulin pathway, linking size to nutrition and hence to the environment. Because of this the study of environmental responses of FA may ultimately be best served by using multivariate size-based measures of FA (i.e., centroid size FA) while at the same time making sure to collect enough samples to accurately estimate the mean.

In conclusion, multivariate size FA may be the better metric for large studies interested in the effects of environmental factors upon FA. Where data is harder to come by (e.g., vertebrate field studies), multivariate shape FA may perform better with the

caveat that shape and pattern are less likely to vary in a population than does size.

Because centroid size must be calculated in order to derive Procrustes distance, both measures can easily and should be examined together.

Does rapid growth stabilize or destabilize development?

The effects of temperature and growth rate on FA appear to support the proximate model which predicts that FA declines with increasing growth rates (Figure 4-3). Aphids from the Gainesville clone decrease mean FA in response to increased temperature and growth rate. It is likely that the Lake Alfred clone is under-sampled and therefore estimates of mean FA are not accurate in that sample. The results of the Gainesville clone, which was sampled adequately, suggests that the prediction of proximate models of the basis of FA (Emlen et al. 1993, Graham et al. 1993), that rapid growth should decrease FA holds true. Møller's hypothesis that rapid growth is stressful because of incurred energetic costs does not appear to hold in the case of aphids. Of course aphids, being phloem feeders, generally have access to more water and carbon than they ever need. This is evidenced by analysis of honeydew composition in this and many other aphid species. Growth and reproduction in aphids is probably more limited by nitrogen than by water or energy (carbon). So it would seem that this system may not be a very good one in which to assess Møller's hypothesis directly. It should be further investigated whether FA of sexually selected traits in energetically limited, genetically diverse populations is positively associated with growth rate as is predicted by the ultimate or evolutionary model presented in Chapter 4.

Can fluctuating asymmetry be a sexually selected trait?

Given that a genetically altered population (chapter 3) demonstrates a consistent response in the shape of the FA distribution does suggest that a potentially strong genetic

basis for FA exists, but is not easily observable through levels of mean FA. This implies some heritability exists and possibly opens the door for selection to act upon FA in the context of mate choice. However, in the future it must be demonstrated, with appropriate sample sizes, that the level of FA in the laboratory can be altered by selection for increased or decreased FA. The opposing predictions of the proximate or mechanistic and ultimate (evolution through sexual selection) explanations of FA, regarding the relationship of temperature, growth rate and FA may offer a method for detecting sexual selection upon FA (chapter 4). If FA has evolved as an indicator of good genes, and hence has related energetic costs, the expectation that FA should increase with growth rate and temperature (in ectotherms) is plausible. Otherwise, if FA is caused by random accumulation of error during development, then the expectation is reversed. FA should decrease with growth rate and temperature as I have demonstrated in a clonal population of aphids that are not energetically limited (chapter 4).

Is fluctuating asymmetry a valuable environmental bioindicator?

Given that the genetic structure of a population (chapter 3) has potentially strong effects upon the shape and location (mean) of the distribution of FA, the usefulness of FA as a bioindicator of environmental stress has to be questioned. Average levels of FA of populations would be difficult to interpret or compare without additional information regarding genetic heterogeneity. However, provided that the study of FA and population genetics were undertaken simultaneously, this problem could be avoided. So FA could still be of use in this regard, however its expense and ease of use compared to other bioindicators would need to be reassessed.

Scaling Effects in Statistical Distributions: The Bigger Picture

This dissertation demonstrates that underlying distributions of some biological data can contain partial self-similarity or power-law scaling. The proper model for describing data such as this sits at a midpoint between those models used in classical statistics and those of statistical physics: Levy statistics (Bardou et al. 2003). To my knowledge, this work represents the first application of such a model in biology.

The sources of power-law scaling in the natural sciences are diverse. Sornette (2003) outlines 14 different ways that power-laws can be created, some of which are very simple. The hypothesis that all power-law scaling in nature is due to a single phenomena such as self-organized criticality (SOC) (Bak 1996, Gisiger 2000) or highly optimized tolerance (HOT) (Newman 2000) is unlikely. Reed (2001) suggests that the model I have used here, stochastic proportional growth that is observed randomly, may explain a great deal of power-law scaled size distributions formerly speculated to have a single cause like SOC or HOT. These phenomena include distributions of city size (Zipf's law), personal income (Pareto's Law), sand particle size, species per genus in flowering plants, frequencies of words in sequences of text, sizes of areas burnt in forest fires, and species body sizes, just to name a few examples.

One of the most common ways that power-laws can be obtained is by combining exponential functions. This effect is also observed when positive exponential/geometric/proportional growth is observed with a likelihood described by a negative exponential function such as in Reed and Jorgensen's (2004) model for generating size distributions. Power laws generated by combining exponential functions are also present in the statistical mechanics of highly interactive systems (e.g., SOC) where the correlation in behavior between two nodes or objects in an interaction network or lattice decreases

exponentially with the distance between them while the number of potential interaction paths increases exponentially with the distance between them (Stanley 1995). In Laplacian fractals, or diffusion limited aggregations observed in chemical electrodeposition and bacterial colony growth (Viscek 2001) there may be a similar interplay between exponential growth (doubling) and the diffusion of nutrients supporting growth which are governed by the normal distribution, of the form $y = e^{-x^2}$.

The exponential function holds a special place in the natural sciences. Any frequency dependent rate of change in nature, or in other words, any rate of change of something that is dependent on the proportion of that something present at that time, is described by the exponential function. Therefore it finds application to many natural phenomena including behavior of populations, chemical reactions, radioactive decay, and diffusion just to name a few. It seems only fitting that many of the power-laws we observe in the natural sciences probably owe their existence to the interplay of exponential functions, one of the most common mathematical relationships observed in nature.

As far as we can ascertain from the recording of ancient civilizations, human beings have been using numbers for at least 5000 years if not longer. And yet the concepts of probability are a relatively recent human invention. The idea first appears in 1545 in the writings of Girolamo Cardano and is later adopted by the mathematicians, Galileo, Fermat, Pascal, Huygens, Bernoulli and de Moivre in discussions of gambling over the next several hundred years. The concepts of odds and of random chance are not generalized until the early twentieth century by Andreyevich Markov and not formalized into mathematics until the work of Andrei Kolmogorov in 1946.

The role of uncertainty in nature is yet to be resolved. Does uncertainty lie only with us or does it underlie the very fabric of the cosmos? Most 19th century scientists (excepting perhaps Darwin) believed that the universe was governed by deterministic laws and that uncertainty is solely due to human error. The first application of statistical distributions by Carl Frederick Gauss and Pierre Simon Laplace were concerned only with the problem of accounting for measurement error in astronomical calculations. The more recent view, that uncertainty is something real, was largely the work of early twentieth century quantum theorists Werner Heisenberg and Erwin Schrodinger and the statistical theory embodied in the work of Sir Ronald Fisher. The basic conceptual revolution in modern physics was that observations cannot be made at an atomic level without some disturbance, therefore while one might observe something exactly in time, one cannot predict how the act of observing will affect the observed in the future with any degree of certainty (at least at very small scales). This is Heisenberg's Uncertainty or Indeterminacy Principle.

Scientists observe natural "laws" only through emergent properties of many atoms observed at vastly larger scales where individual behavior is averaged into a collective whole. Jakob Bernoulli's Law of Large Numbers, Abraham de Moivre's bell shaped curve, and Sir Ronald Fisher's estimation of the mean are also examples of how scientists rely upon emergent properties of large systems of randomly behaving things in order to make sense of what is thought to be fundamentally uncertain world. However, this probabilistic view of the natural world has been challenged in recent decades by some mathematicians who are again championing a deterministic view of nature. Observations by Edward Lorenz, Benoit Mandelbrot and others, of simple and purely deterministic

equations that behave in complex unpredictable ways, has led to a revival in the deterministic view among mathematicians; in this case, uncertainty is a product of human inability to perceive systems that are extremely sensitive to initial starting conditions. For this reason, this new view is often called “deterministic chaos”. And so the question as to whether uncertainty is real or imagined is yet to be resolved by modern science.

One remarkable observation of this latest revolution in mathematics is the frequent occurrence of scale invariance or power-law scaling in systems that exhibit this sort of complex and unpredictable behavior. And so just as the normal distribution or bell curve is an emergent property governing the random behavior of independent objects, the power-law appears to be an emergent property of nature as well; one that seems not only to often to appear in the behavior of interacting objects (i.e., critical systems) but in systems where growth is randomly observed as well. Statistical physics now recognizes two classes of “stable laws”, one that leads to the Gaussian or normal distribution and another that is Levy or power-law distributed. In the former class, emergent behavior is governed by commonly occurring random events while in the latter class the behavior of the group is governed by a few rarely occurring random events. As I have already reviewed earlier, we find that convergence to the mean under these two frameworks can be radically different. Yet both are present in the natural world, and as I have shown in my work, both of these classes of behavior can underlie naturally occurring distributions, causing partial scale invariance in real data. It is my conviction that the biological sciences must in the future adopt the statistical methods of working under both of these frameworks and not simply make assumptions of normality whenever and wherever random events are found to occur.

APPENDIX A
LANDMARK WING VEIN INTERSECTIONS CHOSEN FOR ANALYSIS OF
FLUCTUATING ASYMMETRY

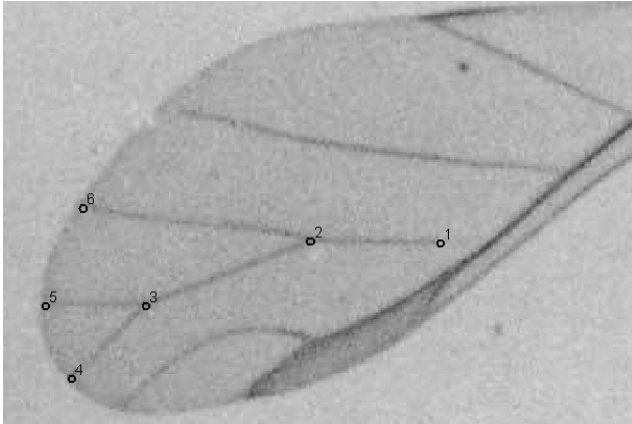


Figure A1. Six landmark locations digitized for *Aphis gossipyii*

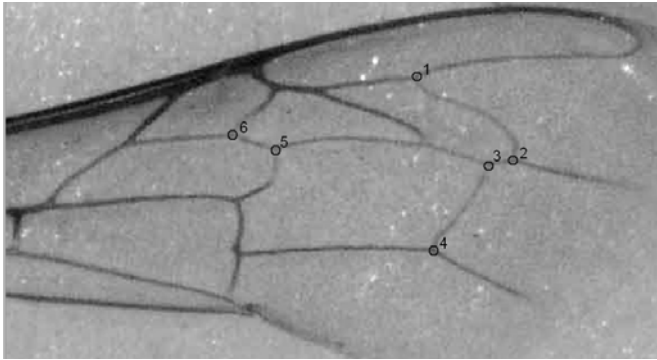


Figure A2. Six landmark locations digitized for *Apis mellifera*

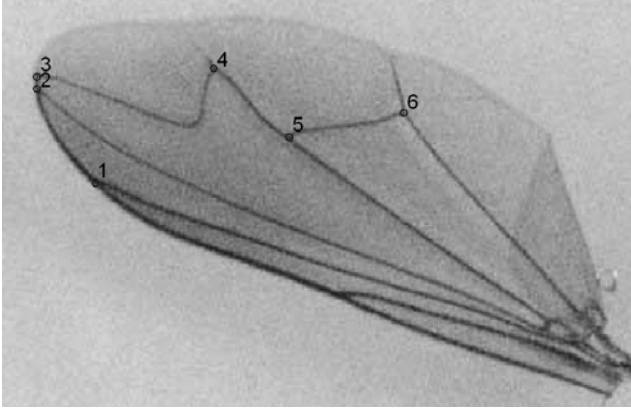


Figure A3. Six landmark locations digitized for *Chrysosoma crinitus*

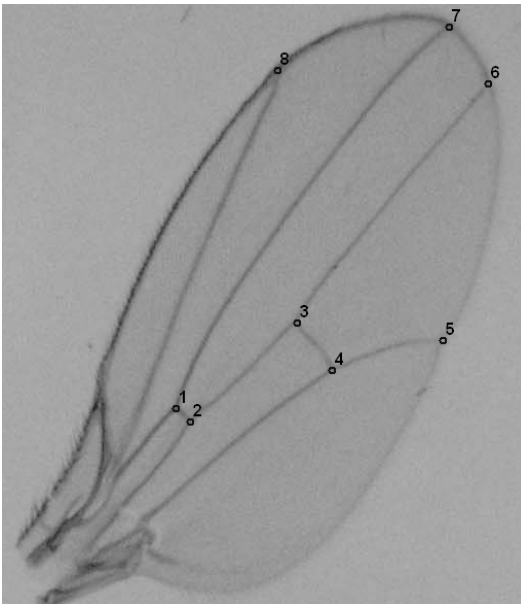


Figure A4. Eight landmark locations digitized for *Drosophila simulans*

APPENDIX B USEFUL MATHEMATICAL FUNCTIONS

The following is a list of the probability density functions for candidate models of the distribution of fluctuating asymmetry. Log likelihood forms of these functions were maximized to obtain best fitting parameters of each model for our data.

Asymmetric Laplace Distribution

(see Kotz et al. 2001)

$$f(x) = \left(\frac{1}{\sigma}\right)\left(\frac{\kappa}{1+\kappa^2}\right)e^{\left(-\frac{\kappa}{\sigma}(x-\theta)\right)} \text{ for } x \geq \theta$$

$$f(x) = \left(\frac{1}{\sigma}\right)\left(\frac{\kappa}{1+\kappa^2}\right)e^{\left(\frac{1}{\kappa\sigma}(x-\theta)\right)} \text{ for } x < \theta$$

where θ = location, σ = scale and κ = skew index (Laplace when $\kappa = 1$)

Half-Normal Distribution

$$f(x) = \left(\sqrt{\frac{2}{\pi}}\right)\left(\frac{1}{\theta}\right)e^{-\left(\frac{1}{2}\right)\left(\frac{x-\mu}{\theta}\right)^2}$$

where μ = minimum data value and θ = dispersion

Lognormal Distribution

(see Evans 2000 or Limpert et al. 2001)

$$f(x) = \frac{1}{x\tau(2\pi)^{1/2}}e^{-(\log x - \nu)^2 / 2\tau^2}$$

where ν = location and τ = shape or multiplicative standard deviation

Double Pareto Lognormal Distribution

(see Reed and Jorgensen 2004)

$$f(x) = \frac{1}{x} \cdot g(\log(x))$$

given the normal-Laplace distribution

$$g(y) = \frac{\alpha\beta}{\alpha+\beta} \cdot \phi\left(\frac{y-\nu}{\tau}\right) \cdot \left[R\left(\alpha \cdot \tau - \frac{y-\nu}{\tau}\right) + R\left(\beta \cdot \tau + \frac{y-\nu}{\tau}\right)\right]$$

where the Mill s ratio $R(z)$ is

$$R(z) = \frac{1 - \Phi(z)}{\phi(z)}$$

and where Φ is the cumulative density function and ϕ is probability density function for standard normal distribution $N(0,1)$, where α and β are parameters that control power-law scaling in the tails of the lognormal distribution.

The limiting forms of the double Pareto lognormal are the left Pareto lognormal ($\alpha = \infty$), right Pareto lognormal distributions ($\beta = \infty$), and lognormal distributions ($\alpha = \infty, \beta = \infty$) with Pareto tails on only the left side, only the right side, or on neither side, respectively.

A description of Reed and Jorgensen's generative model of double Pareto lognormal size distribution.

Reed and Jorgenson's (2004) generative model begins with the Ito stochastic differential equation representing a geometric Brownian motion given below.

$$dX = \mu X dt + \sigma X dw$$

with initial state $X(0) = X_0$ distributed lognormally, $\log X_0 \approx N(v, \tau^2)$. After T time units the state $X(T)$ is also distributed lognormally with $\log X(T) \approx N(v + (\mu - \sigma^2/2)T, \tau^2 + \sigma^2 T)$.

The time T , at which the process is observed, is distributed with density $f_T(t) = \lambda e^{-\lambda t}$ where λ is a constant rate. The double Pareto lognormal distribution is generated when geometric Brownian motion is sampled repeatedly at time t with a negative exponential probability.

LIST OF REFERENCES

- Albert R. and A-L. Barabasi. 2002. Statistical mechanics of complex networks. *Reviews of Modern Physics*. 74: 47-97.
- Babbitt G .A., R.A. Kiltie and B. Bolker. 2006 Are fluctuating asymmetry studies adequately sampled? Implications of a new model for size distribution. *American Naturalist* 167(2):230-245.
- Babbitt G.A. in press. Inbreeding reduces power-law scaling in the distribution of fluctuating asymmetry: an explanation of the basis of developmental instability. *Heredity*
- Baish J.W and R.K. Jain. 2000. Fractals and cancer. *Cancer Research* 60: 3683-3688
- Bak P. 1996. *How Nature Works, the Science of Self Organized Criticality*. Copernicus. New York.
- Balanda K.P. and H.L. MacGillivray. 1988. Kurtosis: a critical review. *The American Statistician* 42(2):111-119.
- Bardou F., J.P. Bouchard, A. Aspect and A. Cohen-Tannoudji. 2003. *Levy statistics and laser cooling: How rare events bring atoms to rest*. Cambridge University Press.
- Bjorksten T.A., K. Fowler and A. Pomiankowski. 2000. What does sexual trait FA tell us about stress? *Trends in Ecology and Evolution* 15(4) 163-166.
- Bookstein F.L. 1991 *Morphometric tools for landmark data: geometry and biology*. Cambridge University Press
- Burnham K.P. and D.A. Anderson. 1998. *Model Selection and Multimodel Inference: a Practical Information – Theoretical Approach*. Springer. New York, NY.
- Carchini G., F. Chiarotti , M.D. Domenico , M. Mattoccia , and G. Paganotti. 2001. Fluctuating asymmetry, mating success, body size and heterozygosity in *Coenagrion scitulum*. *Animal Behavior* 61:661-669.
- Chapman J.W. and D. Goulson. 2000. Environmental versus genetic influences on fluctuating asymmetry in the house fly, *Musca domestica*. *Biological Journal of the Linnean Society* 70(3):403-413.

- Clarke G.M. 1993. The genetic basis of developmental instability: relationships between stability, heterozygosity and genomic co-adaptation. *Genetica* 89: 15-23.
- Clarke G.M. G.W. Brand and M.J. Whitten. 1986. Fluctuating asymmetry – a technique for measuring developmental stress caused by inbreeding. *Australian Journal of Biological Sciences* 39(2): 145-153.
- Clipsham R. Y.H. Zhang, B.L. Huang and E.R.B. McCabe. 2002. Genetic network identification by high density multiplexed reverse transcriptional (HD-MRT) analysis in steroidogenic axis model cell lines. *Molecular Genetics and Metabolism* 77 : 159-178.
- Conlin I. and M. Raff. 1999. Size control in animal development. *Cell* 96:235-244.
- Crow J.F. and M. Kimura 1970. *An Introduction to Population Genetics Theory*. Harper and Row. New York.
- Day S J and P.A. Lawrence. 2000. Measuring dimensions: the regulation of size and shape. *Development* 127:2977-2987
- Debat V. and P. David. 2001. Mapping phenotypes: canalization, plasticity and developmental stability. *Trends in Ecology and Evolution* 16(10) 555-561.
- Diaz B. and E. Moreno. 2005. The competitive nature of cells. *Experimental Cell Research* 306:317-322.
- Ditchkoff S.S., R.L. Lochmiller, R.E. Masters, W.R. Starry and D.M. Leslie jr. 2001. Does fluctuating asymmetry of antlers in White tailed deer (*Odocoileus virginianus*) follow patterns predicted for sexually selected traits? *Proc. R. Soc. London Ser. B* 268:891-898.
- Emlen J.M , Freeman D.C. and J.H. Graham. 1993. Nonlinear growth dynamics and the origin of fluctuating asymmetry. *Genetica* 89: 77-96.
- Evans, M, N. Hastings, B. Peacock. 2000. *Statistical Distributions*. John Wiley and Sons NY.
- Fowler K. and M.C. Whitlock. 1994. Fluctuating asymmetry does not increase with moderate inbreeding in *Drosophila melanogaster*. *Heredity* 73: 373-376.
- Fuller R.C. and D. Houle. 2003. Inheritance of developmental instability. In *Developmental Instability: Causes and Consequences* Edited by M. Polak 2003. Oxford University Press.
- Fragesyi A., D. Gisselsson, F. Mitelman and M. Hoglund. 2003. Power law distribution of chromosomal aberrations in cancer. *Cancer Research* 63: 7094-7097.

- Gangestad S.W. and R. Thornhill. 1999. Individual differences in developmental precision and fluctuating asymmetry: a model and its implications. *Journal of Evolutionary Biology* 12(2): 402-416.
- Gisiger T. 2001. Scale invariance in biology: coincidence or footprint of a universal mechanism? *Biological Reviews* 76:161-209.
- Graham J.H. 1992. Genomic coadaptation and developmental stability in hybrid zones. *Acta Zoologica Fennica* 191:121-131.
- Graham J.H., D.C. Freeman and J.M. Emlen 1993. Antisymmetry, directional asymmetry and dynamic morphogenesis. *Genetica* 89:121-137.
- Graham J.H., K. Shimizu, J.C. Emlen, D.C. Freeman. and J. Merkel. 2003. Growth models and the expected distribution of fluctuating asymmetry. *Biological Journal of the Linnean Society* 80: 57-65.
- Hammer Ø. 2002. PAST version 0.98 statistical software Palaontologisches Institut und Museum, Zurich <http://folk.uio.no/ohammer/past> . Last accessed in April 2004.
- Hardersen S. and C. Frampton. 2003. The influence of differential survival on the distribution of fluctuating asymmetry – a modeling approach. *Journal of Theoretical Biology* 224: 479-482.
- Hilborn D. and M. Mangel. 1998. *The Ecological Detective*. Princeton University Press, Princeton, NJ.
- Hoffman A.A. and R.E. Woods. 2003. associating environmental stress with developmental stability: patterns and problems. In *Developmental Instability: Causes and Consequences*. Edited by M. Polak 2003. Oxford University Press.
- Hogg I.D., Eadie J.M., D.D. Williams and D. Turner. 2001. Evaluating fluctuating asymmetry in a stream dwelling insect as an indicator of low level thermal stress: a large scale field experiment. *Journal of Applied Ecology* 38(6): 1326-1339.
- Houle D. 1989. Allozyme associated heterosis in *Drosophila melanogaster*. *Genetics* 123:789-801.
- Houle D. 2000. A simple model of the relationship between asymmetry and developmental stability. *Journal of Evolutionary Biology* 13: 720-730.
- Kersting U., S. Satar and N. Uygun. 1999. Effect of temperature on development rate and fecundity of apterous *Aphis gossypii* Glover reared on *Gossypium hirsutum* L. *Journal of Applied Entomology* 123:23-27.
- Klingenberg C.P. 2003. A developmental perspective on developmental instability: theory, models and mechanisms In *Developmental Instability: Causes and Consequences*. Edited by M. Polak 2003. Oxford University Press.

- Klingenberg C.P. and G.S. McIntyre. 1998. Geometric morphometrics of developmental instability: analyzing patterns of fluctuating asymmetry with Procrustes methods. *Evolution* 52(5) 1363-1375
- Klingenberg C.P. and H.F. Nijhout. 1999. Genetics of fluctuating asymmetry: a developmental model of developmental instability. *Evolution* 53(2) : 358-375.
- Koehn R.K. and B.L. Bayne. 1989. Towards and physiological and genetical understanding of the energetics of the stress response. *Biological Journal of the Linnean Society* 37: 157-171.
- Kotz S., T.J. Kozubowski , and K. Podgorski. 2001. *The Laplace Distribution and Generalizations: a Revisit with Applications to Communications, Economics, Engineering and Finance*. Birkhauser (c/o Springer-verlag), Boston.
- Kozubowski T. J., and K. Podgorski. 2001. Asymmetric Laplace laws and modeling financial data. *Mathematical and computer modeling* 34:1003-1021.
- Kozubowski T. J., and K. Podgorski. 2002. Log-Laplace distributions, technical report no. 60, Department of Mathematics, University of Nevada at Reno.
- Leamy L. J. 2003. Dominance, epistasis and fluctuating asymmetry. In *Developmental Instability: Causes and Consequences*. Edited by M. Polak 2003. Oxford university Press.
- Leamy L. J. and C. P. Klingenberg. 2005. The genetics and evolution of fluctuating asymmetry. *Annual Review of Ecology, Evolution and Systematics*. 36:1-21.
- Leary R.F., F.W. Allendorf, K.L. Knudsen. 1983. Developmental stability and enzyme heterozygosity in rainbow trout. *Nature* 301: 71-72.
- Leary R.F., F.W. Allendorf, K.L. Knudsen. 1984. Superior developmental stability of heterozygotes at enzyme loci in Salmonid fishes. *American Naturalist* 124: 540-551.
- Lens L., S. Van Dongen and E. Matthysen. 2002. Fluctuating asymmetry as an indicator of fitness: can we bridge the gap between studies? *Biological Reviews* 77:27-38.
- Lerner I.M. 1954. *Genetic Homeostasis*, Oliver and Boyd, London.
- Limpert E. W.A. Stahel and M. Abbot. 2001. Lognormal distributions across the sciences: keys and clues. *Bioscience* 51(5) 341-352.
- Ludwig 1932. *Das rechts-links problem im tierreich und beim Menschen* Springer Berlin.
- MathCad 2001 Mathsoft Engineering and Education Inc. 101Main Street, Cambridge MA 02142 USA

- Mather K. 1953. Genetical control of stability in development. *Heredity* 7: 297-336.
- McCoy K. A. and R.N. Harris. 2003. Integrating developmental stability analysis and current amphibian monitoring techniques: an experimental evaluation with the salamander *Ambystoma maculatum*. *Herpetologia* 59: 22-36.
- Mendes R.L., Santos A.A. Martins M.L. and Vilela M.J. 2001. Cluster size distribution of cell aggregates in culture. *Physica A* 298:471-487
- Merila J. and M. Bjorklund. 1995. Fluctuating asymmetry and measurement error. *Systematic Biology* 44: 97-101.
- Messier S. and J. Mitton. 1996. Heterozygosity at the malate dehydrogenase locus and developmental homeostasis in *Apis mellifera*. *Heredity* 76:616-622.
- Milan M, S. Campuzano and A. Garcia-Bellido 1995. Cell cycling and patterned cell proliferation in the wing primordium of *Drosophila*. *Proceedings of the National Academy of Sciences* 93:640-645.
- Milton C.C., B. Huynh, P. Batterham , S.L. Rutherford and A.A. Hoffman. 2003. Quantitative trait symmetry independent of Hsp90 buffering: Distinct modes of genetic canalization and developmental stability. *Proceedings of the National Academy of Sciences* 100(23) 13396-13401.
- Mitton J.B. and M.C. Grant. 1984. Associations among protein heterozygosity, growth rate and developmental homeostasis. *Annual Reviews of Ecology and Systematics* 15:479-499.
- Mitzenmacher M. (Draft manuscript) A brief history of generative models for power-law and lognormal distribution. Harvard university.
- Moller A.P. 1990. Fluctuating asymmetry in male sexual ornaments may reliably reveal male quality. *Animal Behavior* 40:185-1187.
- Moller A.P. and A. Pomiankowski 1993. Fluctuating asymmetry and sexual selection. *Genetica* 89: 267-279.
- Moller A. P. and J. P. Swaddle. 1997. *Asymmetry, Developmental Stability and Evolution*. Oxford University Press.
- Montroll E.V. and M.F. Shlesinger. 1982. On 1/f noise and other distributions with long tails. *Proceedings of National Academy of Sciences* 79:3380-3383.
- Montroll E.V. and M.F. Shlesinger M.F. 1983. Maximum entropy formalism, fractals, scaling phenomena and 1/f noise: a tale of tails. *Journal of Statistical Physics* 32(2)209-230.

- Mosteller F and J.W. Tukey. 1977. Data Analysis and Regression. Addison-Wesley. Reading MA.
- Mpho M, A. Callaghan and G.J. Holloway. 2002. Temperature and genotypic effects on the life history and fluctuating asymmetry in a field strain of *Culex pipiens*. *Heredity* 88:307-312.
- Newman N. 2000. The power of design. *Nature* 405:412-413.
- Nijhout H.F. 2003 The control of body size in insects. *Developmental Biology* 261:1-9
- Oltvai Z.N. and A-L Barabasi. 2002. Life's complexity pyramid. *Science* 298:763-764.
- Palmer A.R. and C. Strobeck. 1986. Fluctuating asymmetry: measurement, analysis , patterns. *Annual reviews in Ecology and Systematics* 17:391-421.
- Palmer A.R. and C. Strobeck. 2003. Fluctuating asymmetry studies revisited. In *Developmental Instability: Causes and Consequences*. Edited by M. Polak (2003) Oxford University Press.
- Parsons P. A. 1992. Fluctuating asymmetry, a biological monitor of environmental and genomic stress. *Heredity* 68:361-364.
- Perfectti F. and J.P.M. Camachi. 1999. Analysis of genotypic differences in developmental stability in *Annona cherimola*. *Evolution* 53(5) 1396-1405.
- Pinheiro J. and D.M. Bates. 2000. *Mixed-effects Models in S and S-PLUS*. Springer, New York.
- Polak M, A.P. Moller, S.W. Gangestad, D.E. Kroeger, J.T. Manning and R. Thornhill. 2003. Does an individual asymmetry parameter exist? A meta-analysis. In *Developmental Instability: Causes and Consequences*. Edited by M. Polak (2003) Oxford University Press.
- Quandt R.E. 1966. Old and new methods of estimation and the Pareto distribution. *Proceedings of Royal Statistical Society* 1966:55-75.
- Radwan J. 2003. Inbreeding not stress increases fluctuating asymmetry in the bulb mite. *Evolutionary Ecology Research* 5(2) 287-295.
- Raff M. 1992. Social controls on cell survival and cell death. *Nature* 356 April 2 1992 p397-400
- Rao G.Y., S. Anderson and B. Widen. 2002. Flower and cotyledon asymmetry in *Brassica cretica*: genetic variation and relationships with fitness. *Evolution* 56 : 690-698.

- Rasmuson M. 2002. Fluctuating asymmetry – indicator of what? *Hereditas* 136(3) : 177-183.
- Reed W. J. 2001. The Pareto, Zipf and other power-laws. *Economics Letters*, 74: 15-19.
- Reed W. J. and M. Jorgensen. 2004. The double Pareto- lognormal distribution: a new parametric model for size distributions. *Communications in Statistics - Theory and Methods* 33:1733-1753.
- Reeve E.C.R. 1960. Some genetic tests of the asymmetry of sternopleural chaetae number in *Drosophila*. *Genetical Research* 1:151-172.
- Rohlf J. 1999. TPSDIG version 1.31 distributed at SUNY morphometrics <http://life.bio.sunysb.edu/morph/>. Last accessed on June 2003.
- Roman H. E. and M. Porto. 2001. Self generated power-law tails in probability distributions. *Physical Review E*. 63 036128.
- Romeo M., V. Da costa and F. Bardou. 2003. Broad distribution effects in sums of lognormal random variables. *European Journal of Physics B* 32:513-525.
- Ruddon R.W. 1995. *Cancer Biology* 3rd ed. Oxford University Press.
- Rutherford S.L. and S. Linquist. 1998. Hsp90 as a capacitor for morphological evolution. *Nature* 396: 336-342.
- Savage A. and P.J. Hogarth. 1999. An analysis of temperature induced fluctuating asymmetry in *Asellus aquaticus*. *Hydrobiologia* 411:139-143.
- Smith D.R., B.J. Crespi and F.L Bookstein. 1997. Fluctuating asymmetry in the honey bee, *Apis mellifera*: effects of ploidy and hybridization. *Journal of Evolutionary Biology* 10:551-574.
- Sornette D. 2003. *Critical Phenomena in the Natural Sciences: Chaos, Fractals, Self Organization and Disorder: Concepts and Tools*. 2nd ed. Springer, Berlin.
- Stanley H. E. 1995. Power laws and universality. *Nature* 378: p554.
- Thornhill R. and A.P. Moller. 1998. The relative importance of size and asymmetry in sexual selection. *Behavioral Ecology* 9(6):546-551
- Trotta V, F.C.F. Calboli, F. Garoia, D. Grifoni and S Cavicchi. 2005. Fluctuating asymmetry as a measure of ecological stress in *Drosophila melanogaster*. *European journal of Entomology* 102(2):195-200.
- Van Dongen S., W. Talloen and L. Lens. 2005. High variation in developmental instability under non-normal developmental error: a Bayesian perspective. *Journal of Theoretical Biology* 236:263-275.

- Van Valen L. 1962. A study of fluctuating asymmetry. *Evolution* 16 : 125-142.
- Vicsek T. 2001. *Fluctuations and Scaling in Biology*. Oxford University Press.
- Vollestad L A, K. Hindar and A.P. Moller. 1999. A meta-analysis of fluctuating asymmetry in relation to heterozygosity. *Heredity* 83:206-218.
- Waddington C.H. 1942. Canalization of development and the inheritance of acquired characters. *Nature* 150: 563-565.
- Watson P.J. and R. Thornhill. 1994. Fluctuating asymmetry and sexual selection. *Trends in Ecology and Evolution* 9: 21-25.
- West-Eberhard M.J. 2003. Forward. In *Developmental Instability: Causes and Consequences*. Edited by M. Polak 2003. Oxford University Press
- Whitlock M. 1996. The heritability of fluctuating asymmetry and the genetic control of developmental stability. *Proceedings of the Royal Society of London Series B* 263:849-854.
- Whitlock M. 1998. The repeatability of fluctuating asymmetry: a revision and extension. *Proceeding of the Royal society of London Series B Biology* 265:1429-1431.
- Wilson K.G. 1979. Problems in physics with many scales of length. *Scientific American* 241:158-179.
- Woolf C.M. and T. A. Markow. 2003. Genetic models for developmental homeostasis. In *Developmental Instability: Causes and Consequences* Edited by M. Polak 2003. Oxford University Press.
- Xia J.Y., W. Van der Werf and R. Rabbinge. 1999. Influence of temperature on bionomics of cotton aphid, *Aphis gossipyii*, on cotton. *Entomologia Experimentalis et Applicata* 90:25-35.
- Zakharov V.M. and D.V. Shchepotkin 1995. Effect of temperature on developmental stability of silkworm (*Bombyx-mori*) strains differing in heterozygosity level. *Genetika* 31(9):1254-1260

BIOGRAPHICAL SKETCH

Gregory Alan Babbitt received a Bachelor of Arts in zoology from Ohio Wesleyan University in 1989. While working with Dr. Edward H Burt, he co-authored “Occurrence and Demography of Mites in Eastern Bluebird and Tree Swallow Nests,” Chapter 6 in *Bird-Parasite Interactions*, edited by J.E. Loye and M.Zuk. He worked for nine years as a zookeeper and aviculturist at the Columbus Zoological Gardens, designing a successful breeding program for tropical storks, and, during that time, served on the Ciconiiformes Taxon Advisory Group for the American Zoo and Aquarium Association. He received his Master of Science in 2000 from the University of Florida Department of Wildlife Ecology and Conservation. He worked with Dr. Peter Frederick in designing baseline captive reproductive studies of Scarlet Ibises on Disney’s Discovery Island Park that would complement the research group’s ongoing investigations of reproductive failure in ibises in and near Everglades National Park. In 2001, Greg began investigations regarding the underlying basis and proper characterization of developmental instability, the subject of this dissertation work presented here. The second chapter is also published in the February 2006 *American Naturalist* 167(2) pp230-245. The third chapter has been accepted for publication in a future volume of *Heredity*. After receiving his PhD in zoology from the University of Florida, Greg will be starting post-doctoral work with Dr. Yuseob Kim at Arizona State University’s Biodesign Institute in the Center for Evolutionary Functional Genomics.